Winter 12-2-2013

ALTITUDINAL AND THERMAL VARIATION IN AMBIENT NUTRIENT UPTAKE AND UPTAKE KINETICS IN TEMPERATE STREAMS

Brady Kohler

University of Nebraska-Lincoln, kohlerbrady@gmail.com

ALTITUDINAL AND THERMAL VARIATION IN AMBIENT NUTRIENT UPTAKE AND UPTAKE KINETICS IN TEMPERATE STREAMS.

By

Brady S. Kohler

A THESIS

Presented to the Faculty of

The Graduate College at the University of Nebraska

In Partial Fulfillment of Requirements

For the Degree of Master of Science

Major: Natural Resource Sciences

Under the Supervision of Professor Steven A. Thomas

Lincoln, Nebraska

December 2013

ALTITUDINAL AND THERMAL VARIATION IN AMBIENT NUTRIENT UPTAKE AND UPTAKE KINETICS IN TEMPERATE STREAMS.

Brady Scott Kohler, M.S.

University of Nebraska, 2013

Advisor: Steven A. Thomas

Temperature is often considered a master variable controlling many chemical reactions and biological processes. Research efforts have begun address how temperature affects whole stream nutrient uptake rates, but little has attention has been paid to the influence of temperature on nutrient uptake versus concentration kinetics. In this study, we investigated 1) how ambient nutrient uptake rates and 2) nutrient uptake kinetics vary along a thermal gradient established by an altitudinal gradient in the Rocky Mountains, Colorado, USA. Instantaneous nutrient additions were performed at 15 streams within three adjacent drainage basins in the Colorado Rocky Mountains to test these questions. Ambient uptake metrics were estimated using multiple approaches and quantitatively related to variation in ambient temperatures and long-term thermal regimes. We found no relationship among nutrient uptake velocities and temperature. However, NH_4^+ uptake rates significantly increased with temperature whereas NO_3^- uptake rates decreased with temperature, though the significance differed by estimation approach and component of thermal regime examined. Response in uptake to increased nutrient availability was also estimated for each stream, where response in NO_3^- uptake was found to increase with increasing

temperatures. In summary, temperature partially accounted for variation in nutrient uptake rates observed in this study. However, background nutrient concentrations and other stream characteristics also exert control on uptake dynamics and I surmise those controls dampen the role of temperature in controlling uptake rates in these streams.

ACKNOWLEDGEMENTS

I am very thankful for all the folks that helped me throughout the course of my studies here. A big thank you to Steve Thomas for not only allowing me the opportunity to conduct this research, but also facilitating my interest in stream biogeochemistry and providing the many hours of much needed assistance. Thanks to my lab mates, Tom Heatherly, Katie Lawry, and Lavenia Ratnarajah, for putting up with my shenanigans and sharing the many memorable experiences. I would also like to thank Kayce Anderson for her assistance in the field, Keeley MacNeill, Brian Gill, Alisha Shah, and Rachel Harrington for the help and good times in Colorado, and Kiran Singh for her help in the lab, and the many members of our extended UNL lab group for their support. Additionally, thanks to Jonesy for always being there and Tyler Kohler for all his support over the years. Finally, I would like to thank my committee members Dan Snow and Karrie Weber, all the folk in EVOTRAC for their help with this project, and the School of Natural Resources for paying my bills. This study was funded by the National Science Foundation.

TABLE OF CONTENTS

LIST OF TABLES

LIST OF FIGURES

INTRODUCTION

Water is perhaps the most important resource, whether defined by human uses or by the requirements of other organisms. Streams are important ecosystems from both these perspectives; unfortunately they are also among the most degraded aquatic habitats across the globe. Streams receive point sources of pollutants from industrial and agricultural production and non-point loading of nitrogen and phosphorous in both agricultural and urban landscapes. Excessive nutrient loading alters the ability of streams to process and retain nutrients (Mulholland et al. 2008). Understanding the mechanisms that control stream responses to changing nutrient loads is an important research frontier in stream biogeochemistry

Lotic ecosystems differ from their lentic counterparts (eg. lakes and reservoirs) by their unidirectional flow of water. Streams also differ from lentic systems in that much of the biological activity is associated with benthic flora and fauna as opposed to planktonic communities that dominate in lentic systems. The base of the food web in streams is comprised of algae and heterotrophic microorganisms associated with detritus on the stream bed or embedded within biofilms growing on benthic surfaces. These biofilms, referred to collectively as periphyton or epilithon, consist of a complex mixture of algae, bacteria, archaea, fungi, extracellular exudates, and detritus. Water flow and associated turbulence ensures the continuous delivery of dissolved gases, nutrients, and energy to benthic communities, removes metabolic waste, and provides a mechanism for species dispersal (Newbold 1992).

The physical template of streams makes them an extremely 'open' ecosystem compared to closed systems, such as lakes, where material transfers across boundaries are minor compared to internal fluxes. Historically, water flow impeded the study of ecosystem processes such as nutrient cycling in streams. With the development of the Nutrient Spiraling Concept, first proposed by Webster (1975; Webster and Patten 1979), stream ecologists now have both a theoretical and quantitative framework for measuring nutrient cycling in streams and for understanding the factors that control variance in cycling within and among systems (Newbold et al. 1981, 1982a, 1983, Stream Solutes Workshop 1990). The mathematical framework for describing nutrient spiraling begins with the recognition that one elemental cycle occurs over a finite distance, which is referred to as the spiral length (S). Spiral length consists of two distinct phases, the distance travelled as an inorganic compound, called the uptake length (S_W), and the distance associated with organic phases of a nutrient, referred to as the turnover length (S_B). Experimentally determining turnover length for nutrients is inherently difficult due to the various forms organic nutrients take, difficulty in measuring the movement of these forms, and the slow turnover of organic material compared to abiotic forms (Newbold 1992). Thus, most research efforts have quantified uptake lengths rather than the full spiral lengths when comparing and contrasting nutrient spiraling in streams (Mulholland et al. 2000, Webster et al. 2003, Hall et al. 2009, Bott and Newbold 2013).

While many studies in stream biogeochemistry have estimated uptake metrics (Tank et al. 2000, Mulholland et al. 2006, von Schiller et al. 2008, Marti et al.

2009), few have sought to describe the kinetics of biological uptake reacting as communities respond to changes in nutrient supply (but see Kim et al. 1990, Dodds et al. 2002). Recently developed field techniques have begun to allow researchers to do this using a single injection of solutes combined with a dynamic sampling procedure (Payn et al. 2005, Tank et al. 2008, Covino et al. 2010a).

Uptake dynamics are governed by both biotic and abiotic mechanisms. When biological uptake is constrained by the delivery of nutrients to benthic communities through advection and diffusion, the relationship between uptake rate and concentration is expected to be linear (Newbold 1982b, Kim et al. 1992). However, when uptake rates are controlled by enzymatic function and/or physical adsorption to the sediment, uptake is expected to be non-linear with saturation of uptake rates observed as nutrient supply increases (Dodds et al. 2002). Saturation of uptake rates in response to high nutrient availability has been demonstrated in several studies (Payn et al. 2005, Earl et al. 2006, Covino et al. 2010a). Saturation kinetics can be represented using a Michaelis-Menton model, which provides two additional descriptors of nutrient processing: the maximum rate at which nutrients can be incorporated into biomass (U_{max}) and how quickly the biology responds to increases in nutrient availability (K_s).

Global climate change has caused changes in temperature regimes, among other things, and this is likely to continue for the foreseeable future (IPCC 2007). Climate change has the potential to alter nutrient uptake rates through several mechanisms, the most obvious of which is the direct effect of temperatures on the rates of biological activity (the Q10 effect). However, climate change is also

predicted to alter a stream's flow regime with potential consequences for a variety of ecosystem functions, including nutrient uptake. Seasonal temperature variations have been shown to significantly affect stream nutrient uptake dynamics (Valett et al. 2008, von Schiller et al. 2008), however isolating the effect of temperature on nutrient dynamics has proven to be difficult (Marti et al. 2009). Temperature also changes water viscosity and diffusivity, which can impact the delivery of nutrients through benthic boundary layers and alter the flow of water through bed sediments (e.g. the hyporheic zone; see Cardenas and Wilson 2007).

This research focuses on whether existing thermal variation in temperate streams predicts variation in nutrient uptake and uptake kinetics. **My organizing objective is to determine whether ammonium, nitrate, and phosphate uptake systematically vary with altitude and temperature when assessed at the ecosystem scale**. Specifically, this research is designed to answer the following research questions:

1) How do ambient uptake rates of these chemical species vary with altitude and temperature?

And

2) How do altitude and temperature influence the response rate of microbial communities to increased nutrient availability?

I hypothesize that ambient uptake rates will increase with temperature due to the direct influence of temperature on the enzymatic activity of resident microbial communities (i.e. Q10 effect, where the rate of enzymatic activity theoretically doubles with a 10 °C rise in temperature). I also predict that the

kinetics that reflect a communities response to increased nutrients will be dampened (e.g. slower response, lower maximum rates) as temperatures drop with altitude.

METHODS

STUDY SITES

This research was conducted in the summer of 2012 as a subcomponent of a broader NSF funded effort (EVOTRAC) to compare and contrast streams of varying thermal regimes using natural altitude gradients in both temperate (Colorado) and tropical (Ecuador) ecosystems. For this study, only sites in Colorado were addressed and 15 streams were selected from the larger project's sites in the Front Range of Colorado's Rocky Mountains, near Colorado State University in Fort Collins (Table 1). The streams were distributed across three adjacent river basins (Cache la Poudre, Big Thompson, and Saint Vrain) and ranged in altitude from 1992-3478 m, with a targeted vertical separation of ~100 m between each stream. All streams experience little human impact and were located on either National Forest or Rocky Mountain National Park property, with the exception of Black Canyon being on private land.

The winter and spring of 2012 exhibited abnormally dry conditions from limited snowfall and rain events. These conditions, combined with high summer temperatures and thunderstorms, promoted large lightning-induced wildfires in May-June and low summer stream flows across Colorado's Front Range. Streams

included in this study did not experience significant fires in their specific watershed that would impact the water chemistry.

For each stream, reaches of ~200-300 m were identified upstream of any road crossings that had relatively homogenous riparian and channel characteristics, avoiding natural dams and significantly large tributaries. Reach lengths were based on flow velocity and mean solute residence time (see Experimental Design below) and ranged from 66-347 m. All tributaries within the reaches were small and considered negligible. Streambeds were mostly comprised of cobblestones, boulders, and patches of sand. Riparian vegetation varied with altitude: lower altitude streams were generally forested with few overhanging plants, while streams at higher altitudes generally had shrubs and grasses lining the banks.

Temperature

Temperature was measured in each stream using two different approaches. First, a multi-parameter sonde (YSI, Inc., Yellow Springs, OH, USA) was programmed to record temperature every 15 s over the time period that spanned the time when nutrients were added to the top of the study reach and the time when the last downstream sample was collected. From this data-series, the mean water temperature from the duration of the nutrient addition could be quantified. Streams also had multiple temperature loggers (iButtons, iButtonLink, LLC., East Troy, WI, USA) deployed at each site (various depths in each channel) that were installed to quantify long-term temperature patterns (> 1 yr) which had been in place for 9 months at the time of this experiment. The iButtons were programmed to record

temperature measurements every 4 hours. Data retrieved from the iButtons were used to estimate mean, minimum, and maximum water temperatures in each stream for the 10-day period preceding the nutrient release.

Epilithon Collection

In order to account for variation in algal and biofilm standing stocks on nutrient uptake rates in these streams, I sampled epilithon from submerged rocks collected from riffle of each stream, giving an assessment of the algal, plankton, and fungal communities. Rocks were collected from 3 to 5 randomly distributed transects that encompassed the reach used for the nutrient injections. The rocks from each transect were placed in a sampling tray and a wire brush and squirt bottle were used to scrape the biofilm off each rock (resulting in one combined sample per transect). All rocks and brushes were rinsed with stream water and care was taken to collect all of the removed material in a large plastic collection tray. Next, all of the slurry was transferred into a large graduated cylinder and the total volume recorded. The epilithon slurry was then agitated, to promote homogenization, and a subsample was collected on an ashed 25-mm Whatman™ GF/F (Part no: 1825-025, pore size = 0.7μm) filter via a pipette and suction flask. Filters were immediately wrapped in aluminum foil, placed on dry ice, and transferred to a -20 ^{o}C freezer upon returning from the field. Lastly, photographs were taken of each rock on a graduated mat after being scraped. The photos were analyzed in ImageJ (National Institutes of Health, Bethesda, Maryland, USA) to determine planer surface area of each rock, and thus the total planer surface area that produced each slurry.

Chlorophyll **a** abundance was quantified using a fluorometric approach with an acid correction for pheophytin (EPA Method 445.0). Briefly, all filter samples were placed in individual film canisters immediately following their removal from the freezer and tin foil wrapping to prevent photobleaching. Extraction consisted of adding a 10 mL aliquot of 90% ethanol, sealing, and allowing the canisters to sit at room temperature for 24 hours. Immediately following the 24-hr extraction period, the fluorescence of the resulting solution was measured using an Aquafluor® handheld fluorometer (Turner Designs, Sunnyvale, CA, USA: excitation wavelength = 430 nm; emission wavelength = 680 nm). The fluorometer used in this study was calibrated to read in units of μg chlorophyll **a** L^{-1} approximately 1 month prior to the measurements. Benthic standing stock estimates of chlorophyll **a** (μg chl **a** m^{-2}) were determined by multiplying the each slurries concentration (μg chl **a** L^{-1}) by the total slurry volume (L) and dividing by the total rock surface area (m^2).

NUTRIENT UPTAKE MEASUREMENTS

Laboratory Preparation: Prior to going to the field, a predicted response curve was created relating specific conductance (SpC) to NaCl concentration. Specific conductance was measured using a multi-parameter YSI 6920 V2 water probe (YSI Incorporated, Yellow Springs, OH, USA) which is the same instrument used for all field measurements of specific conductance and temperature. Quantifying the NaCl – SpC response curves allowed discharge estimates to be derived quickly in the field from instantaneous NaCl injection using a mass balance approach (see below). An accurate assessment of discharge in the field is critical since quantities of all solutes

to be released were based on the stream's discharge. In this study, we added approximately 25 g NaCl, 100 mg-N L^{-1} NH_4Cl, 200 mg-N L^{-1} $NaNO_3$, and 100 mg-P L^{-1} KH_2PO_4 for every L s^{-1} discharge. By normalizing the proposed increase in nutrient load to discharge, we were able to create similar conditions across streams. Portable scales were unable to be obtained for this experiment so all salts were pre-weighed to various masses and transported to the field in plastic bags. These were combined to produce loading levels close to the target concentrations described above.

Discharge and Experimental Design: At each stream, I identified stream reaches of ~ 200-300 meters above any road crossing and in which riparian conditions were approximately homogeneous. A riffle was identified near the bottom of each reach and the YSI multi-parameter sonde was deployed in a well-mixed area but avoiding overly turbulent water that can create noise in specific conductance readings. Once real-time readings stabilized, the probe was programed to log specific conductance, temperature, and dissolved oxygen every 15 s.

Prior to estimating discharge by NaCl addition, background water samples were collected to quantify ambient nutrient concentrations of NH_4^+, NO_3^-, and soluble reactive phosphorus (SRP) prior to nutrient additions. All water samples were immediately filtered through an ashed, 0.7 μm glass fiber filter (Whatman 25-mm GFF) and the filtrate collected in 20 mL scintillation vials (NO_3^- & SRP) and 30 mL amber HDPE bottles (exactly 10 mL for NH_4^+). Nitrate and SRP samples were immediately placed on dry ice and transferred to a -20 °C freezer immediately following return for the field. Nitrate and SRP samples remained frozen until

analysis at UNL in the fall of 2012. All NH_4^+ were analyzed within 12 hours using the method of Holmes et al (1999) as modified by Taylor et al (2007). Analytical details are described below.

To determine stream discharge, I first visually approximated the amount of flow to determine the amount of NaCl to add to each stream. I then combined pre-weighed bags of NaCl to achieve an instantaneous concentration of ~ 25 g NaCl per 1 L s^{-1} discharge. The known NaCl mass was recorded, emptied into a large bucket filled with stream water, and was stirred until fully dissolved. At a known distance above the multi-parameter sonde (~ 100-200 m), the solution was instantaneously released into the stream by pouring the NaCl 'slug' into the channel and quickly rinsing the bucket with stream water. The location and time of addition was recorded. The addition of salt to the stream creates a detectable change in the streams specific conductance that is proportional to its concentration (based on the predicted response curve described above). By monitoring the specific conductance measured by the multi-parameter sonde, I was able to observe the slug pass by the downstream sampling location. When the entire slug cleared the monitoring location and specific conductance had returned to background conditions, sonde data was uploaded to a field laptop computer. Stream discharge was calculated by background-correcting the specific conductance data, then using those values to estimate tracer NaCl concentration (via the standard curve discussed above), and solving for discharge using the following equation:

Equation 1: $$Q = m_{NaCl} / \Sigma ([NaCl] * \Delta t)$$

where m_{NaCl} is the mass (mg) of NaCl dissolved in the slug, [NaCl] is the concentration (mg L^{-1}) determined by the specific conductance, and Δt is the duration of the time step (15 s). Mean stream velocity was also estimated from the slug addition by dividing the reach length by the time it took to reach maximum specific conductance (Triska et al. 1989). Mean velocity estimates were used to estimate reach lengths of equal residence time (~ 15 minutes) across all study streams. Thus, while reach lengths varied across streams, the period of time added nutrients were in the stream was standardized across our study sites.

Instantaneous Nutrient Additions: Discharge and target concentrations (see above) were used to estimate the amount of nutrients to use at a specific site. Pre-weighed aliquots of nutrients were combined to come as closely to those estimates as possible. We added nutrients all as one cocktail (NH_4Cl, $NaNO_3$, and KH_2PO_4) in order to help isolate the effect temperature on uptake rates and how stream communities respond to increased nutrient supply. The nutrients, as well as the conservative tracer, were added as salts and also affect the specific conductance (SpC) of the stream once fully dissolved and dissociated. However, the mass used of the nutrients was three orders of magnitude lower than that of the conservative tracer, making their effect on SpC negligible. Adding all nutrients together helped to ensure that uptake of one nutrient form was not constrained by the limited availability of another (Schade et al. 2011). While conducting fully-factorial nutrient additions (alone and in all combinations) would have been desirable to help differentiate between uptake of nitrogen and processes such as ammonium

oxidation to nitrate (nitrification) among other things, it would have been impossible in 15 streams given time and other logistical constraints and therefore we focused on an approach that maximized the our ability to assess temperature in as many streams as we could.

Nutrients and salt were added to a large bucket of stream water and mixed until fully dissolved. All nutrient slugs were performed around midday (10:30 am – 12:30 pm) to help account for diurnal variation in light availability and biological activity (Mulholland et al. 2006). When the nutrient slug reached the sampling location, grab samples were collected just upstream (< 1 m) of the multi-parameter sonde at designated time intervals using 60 mL syringes, following the TASCC procedure described by Covino et al. (2010a). More frequent sampling was conducted during times in which the specific conductance was more dynamic to sufficiently describe the breakthrough curve while minimizing the total number of samples collected.

Once the slug had cleared (specific conductance returned to background conditions), sampling was halted and all of the collected water samples were filtered as described above for background nutrient collection. Following the water sample collection period, stream reach length (distance from addition point to multi-parameter sonde) and > 50 stream widths were measured and recorded using a meter tape. The multi-parameter sonde was retrieved prior to leaving, downloaded and data backed-up on the field laptop computer.

Water Chemistry Analysis: Each water sample described above was filtered through an ashed, 0.7 μm glass-fiber filter (Whatman™ 25-mm GF/F) immediately following their collection. For each NH_4^+ sample, 10 mL of the grab sample was dispensed in an amber 30 mL HDPE bottle and doped with a 2.5 mL aliquot of an OPA solution according to the method proposed by Holmes et al. (1999), as modified by Taylor et al. (2007). A set of NH_4^+ standards were also created for each stream in amber 30 mL HDPE bottles using 10 mL of stream water (collected prior to the releases), 2.5 mL OPA solution, and an aliquot of NH_4^+ working stock solution. Standards consisted of one un-doped stream sample (OPA was added immediately before being analyzed to address the background fluorescence and matrix effects of the OPA solution and stream water), a blank (stream water and OPA solution with no added NH_4^+ to account for background NH_4^+ concentrations), and 6 standards of progressively higher NH_4^+ concentrations, encompassing the range of sample concentrations. The OPA solution comprised of ortho-phthalaldahyde (OPA, dissolved in high-grade ethanol to reduce autofluorescence), which binds to NH_4^+ creating a fluorescent chemical species, sodium sulfite (dissolved in ultrapure water), which inhibits OPA's ability to bind to any amino acids that may be present in the solution, and a sodium tetraborate buffer (dissolved in ultrapure water). The samples and standards were allowed to react at ambient temperatures for 6-8 hours, where the fluorescence is most stable, before being analyzed using a handheld fluorometer (Turner Designs AquaFluor®).

Samples for NO_3^- and SRP were temporarily stored in a cooler of ice or dry ice and were frozen as soon as possible in freezers at Colorado State University.

After completing the field season, they were brought to the University of Nebraska and analyzed in tandem via colorimetric techniques on a QuickChem autoanalyzer (Lachat Instruments, Chicago, IL, USA). A series of 6 “double-standards” (containing known quantities of both NO_3^- and PO_4^{3-}, encompassing the range of sample concentrations) and a blank were used to create a standard curve for each analyte. Five background samples were analyzed and averaged from each stream to estimate ambient concentrations of both NO_3^- and SRP. Nitrate concentrations were quantified by first reducing NO_3^- to nitrite (NO_2^-) by running the samples through a column containing copper-cadmium granules (regenerated each day using a dilute copper sulfate solution). The nitrite (combined NO_3^- and background NO_2^-) is then reacted with sulfanilamide and N-(1-naphthyl)-ethylenediamine dihydrochloride (NED) to yield an azo dye that can be analyzed colorimetrically. Nitrite concentrations were determined by the absorbance of the resulting azo dye at 520 nm in accordance to the Beer-Lambert law. Nitrate concentrations were separated from total NO_2^- for the samples by bypassing the cadmium column and obtaining a background NO_2^- concentration (a constant for each stream) that could be subtracted from the total NO_2^- estimates (Lachat Method 10-107-04-1-Q, EPA/600/R-93/100 – EPA Method 353.2). Soluble reactive phosphorous concentrations were quantified by reacting ortho-phosphate (PO_4^{3-}) with an acidified solution of ammonium molybdate and antimony potassium tartrate to yield an antimony-phospho-molybdate complex. This complex is then reduced via ascorbic acid to form a blue solution that can be analyzed colorimetrically by its

absorbance at 880 nm in accordance to the Beer-Lamber law (MCAWW EPA/600/4-79/020 – EPA Method 365.3).

TRANSIENT STORAGE

Streams have complex flow and simple advection and dispersion models are often inadequate in predicting salt and nutrient breakthrough curves (BTCs). Advection and dispersion models that include transient storage functions like those developed by Bencala and Walters (1983) better reflect BTC data. The transient storage zone represents a non-advective volume where solutes are temporarily retained. These volumes might be within the stream channel (lateral eddies and/or pools) or within the streambed (hyporheic zones). Longitudinal movement in transient storage zone are very slow compared to the main channel and assumed to be zero in transient storage models. The effect of transient storage zones on solute transport can lead to a visible asymmetry in BTCs, where solute concentrations will rapidly approach a maximum before slowly returning back to ambient levels. The extent of the asymmetry is largely dependent on the size of the transient storage zone as well as the rate of solute exchange between the main channel and storage compartments.

For each of my streams, I applied the One-dimensional Transport with Inflow and Storage (OTIS) model (Runkel et al. 1998) to the conservative tracer (Cl^-) data to estimate each stream's hydrological characteristics. OTIS estimates conservative transport by simultaneously solving a pair of partial differential equations that

describe advection and dispersion forces within the main channel and exchange between the main channel and a transient storage zone:

Equation 2a: $$\frac{\partial C}{\partial t} = \frac{Q}{A}\frac{\partial C}{\partial x} + \frac{1}{A}\frac{\partial}{\partial x}\left(AD\frac{\partial C}{\partial x}\right) + \frac{q_{lin}}{A}(C_L - C) + \alpha(C_S - C)$$

Equation 2b: $$\frac{\partial C_S}{\partial t} = \alpha\frac{A}{A_S}(C - C_S)$$

where A and A_S are the cross-sectional area of the main channel and storage zone, respectively, C, C_L, and C_S are the concentration of the solute in the main channel, lateral inflow, and storage zone, respectively, D is the dispersion coefficient, Q is the discharge of the stream, q_{lin} is the lateral inflow rate, t is the time since release, x is the reach length or distance from release point, and α is the exchange coefficient between the main channel and storage zone. Best model fits were achieved by (a) manually fitting the model to the observed chloride BTC concentrations and (b) using the resulting coefficients to seed the OTIS optimization package (OTIS-P) which optimizes model coefficients by minimizing the squared difference between experimental and simulated values. Simulations yielded estimates for dispersion (D), absolute and relative (to main channel) cross sectional area of the transient storage zone (A_S and A_S/A, respectively), and the exchange rate between the main channel and storage zone (α) since lateral inflow was none or negligible in all streams.

Estimating Ambient Spiraling Metrics

Regressive Approach: Nutrient additions were performed in accordance to the TASCC procedure described by Covino et al. (2010a). Briefly, a single simultaneous

release of a conservative tracer (NaCl) and three biologically-active nutrients (NH_4^+, NO_3^-, and PO_4^{3-}) was performed at each stream to quantify uptake dynamics. As this "slug" passed the sampling location, the resulting breakthrough curve was described by both monitoring specific conductance and collecting grab samples, which were later analyzed for their chemical composition (see above Water Chemistry Analysis), at specific time intervals (Figure 1). Using the change in each nutrient:tracer ratio between the slug and every grab sample, a specific uptake value could be determined for each sample relating its uptake to its respective analyte concentration. The resulting uptake versus concentration values for each stream could then be used to estimate its ambient uptake.

Three spiraling metrics were calculated to describe uptake for each of the added nutrients: uptake length (S_w, m), uptake velocity (V_f, cm s^{-1}), and areal uptake rate (U, μg m^2 s^{-1}). For all streams and for each nutrient form, uptake metrics were calculated for each time point in the breakthrough curve in order to examine how these metrics change as concentrations rise and fall. Metrics were estimated by first calculating the longitudinal loss rate (k_L, m^{-1}) of a specific nutrient, which is equal to the slope of the linear relationship between ln-transformed background corrected nutrient:tracer ratio at the injection point (a constant) and that which occurred at the sampling location against reach length (Figure 2). The inverse of k_L is defined as the uptake length (S_w, m) and represents the mean distance travelled by an element prior to being lost from the water column. Each stream's ambient uptake length was then determined by plotting the individual uptake lengths against their respective nutrient concentration and extrapolating the linear regression to ambient

conditions using standard procedures that correct for background activity (Figure 3)(Payn et al 2005).

Ambient uptake lengths can be heavily influenced by the rate of stream flow, making it a poor metric to use to compare across streams of different sizes. Therefore, uptake lengths are often converted to uptake velocities (V_f), which normalizes uptake lengths for stream discharge using:

Equation 3: $$V_f = Q / (S_w * w)$$

where Q is stream discharge and w is the wetted width of the stream. Uptake velocity describes the theoretical rate that the nutrient molecule travels toward its point of uptake. In other ecosystems, uptake rates are often expressed as a mass flux per unit area and a similar calculation can be made in streams. Areal uptake rates (U, M $L^{-2}T^{-1}$) can be calculated using :

Equation 4: $$U = (Q * C) / (S_w * w) = V_f * C$$

where C is the background concentration of the nutrient in a given stream. Re-arranging the second function of U yields $V_f = U / C$ and highlights why V_f has often been used to describe the efficiency of a system with respect to its ability to remove the nutrient load to which its exposed.

Mass-Balance Approach: Spiraling metrics for each stream were also predicted using a mass-balance approach. Here, uptake is estimated by determining the total mass of nutrient that was "recovered" at the base of the reach, using a time step integration, versus the amount that was added. By relating the fractional loss of mass to distance travelled (reach length), a single uptake length for a given stream

can be quantified. The mass of each nutrient recovered at the bottom of the reach was determined by estimating the area under the nutrient's breakthrough curve (Figure 4) using:

Equation 5: $m_f = Q * \Sigma (C * \Delta t)$

where Q is the discharge of the stream, C is the average concentration of the two grab samples describing that specific time step, and Δt is the integrated time step, determined by the sampling rate (time between grab samples). The recovered mass was then used to calculate uptake length by the equation:

Equation 6: $S_w = L / (\ln(m_i) - \ln(m_f))$

where L is the reach length and m_i and m_f are the initial mass and the mass recovered of the chemical species in consideration, respectively. Uptake length was converted to uptake velocity and areal uptake rate using the same equations as the regressive approach described above.

Uptake Versus Concentration Relationships: Inorganic nutrient molecules can take many different biological and chemical pathways in streams before being removed from water column. Nitrate can be removed by aerobic processes, such as assimilatory nitrate reduction, or anaerobic processes, such as dissimilatory nitrate reduction to ammonium or denitrification. Ammonium can also be removed by aerobic processes, such as nitrification, or anaerobic processes, such as anoxic ammonium assimilation or anammox (conversion of ammonium to dinitrogen gas). Phosphorous can be removed by both biotic and abiotic mechanisms, where sorption to sediments and co-precipitation in the presence of the appropriate metal

(eg. Al, Ca, or Fe) at the right pH can often occur. The biota within a stream can respond differently to increased nutrient availability depending on what forces are constraining nutrient delivery and uptake. Uptake rates can respond linearly with increased nutrient availability when streams are experiencing "pure" nutrient limitation and diffusion is the only constraining force (Newbold 1982b, Kim et al. 1992). However, when nutrient availability exceeds the rate of enzymatic function, uptake will no longer increase linearly and instead approach a maximum rate (Dodds et al. 2002). Target concentrations of the nutrient slug were designed to reach those saturated conditions, so nonlinear uptake response was expected.

Individual uptake rates were calculated for each grab sample using a similar procedure as with whole-stream ambient uptake rates. However, each stream's mean flow velocity, thus discharge, does not effectively relate to each grab sample due to the dynamic sampling across the duration of the experiment. Therefore, instead of using the discharge-based equation described above to convert ambient S_w to U, individual uptake rates were calculated for each sample using:

Equation 7: $$U_{ind} = (L * z * C) / (t * S_w)$$

where L is the reach length, z is the average depth of the stream, C is the geometric mean of the background corrected "expected" concentration (SpC-derived NaCl concentration converted to nutrient concentration via nutrient:tracer ratio in the slug, or rather theoretical nutrient concentration if travelling conservatively) and background corrected measured concentration of the grab sample, t is the time the grab sample was collected (since the release), and S_w is the individual uptake length of the grab sample.

Time-dependent individual uptake rates for each grab sample were added to the stream's ambient uptake rate, yielding the total uptake rate (U_{tot}), and were plotted versus their respective concentration (the geometric mean of the background corrected expected concentration and background corrected measured concentration of the sample, C). Plots were then fit with a Michaelis-Menten curve following the equation:

Equation 8: $$U_{tot} = (U_{max} * C) / (K_s + C)$$

where U_{max} is the uptake rate when the stream reaches saturation and K_s is the concentration of the nutrient when $U_{tot} = ½\ U_{max}$. Plots were also fit with a linear model, in the event that saturation was not achieved and response did not follow Michaelis-Menten kinetics, where the slope of the regression relates to the response in uptake to increased nutrient availability.

Statistical Analysis

The magnitude of how altitude and temperature influenced uptake dynamics and biological response to increased nutrient availability was assessed using generalized linear models (GLMs), linear models, and one-way ANOVAs in the R console, version 2.13.1 (R Development Core Team 2011). Dependent variables included all variations of V_f and U, as well as response slopes for each nutrient (from U vs. C relationships). Before creating GLMs, pair-wise correlations were analyzed between all explanatory variables and factors were removed for autocorrelation (eg. elevation and temperature were not included within the same model). Global models were then created for each dependent variable and were simplified using

backwards selection to obtain the most appropriate explanatory equation. Linear models for altitude, slug temperatures, mean, minimum, and maximum temperatures from the day of the experiment, and mean, minimum, and maximum temperatures from the previous ten days were developed to examine the variance in ambient uptake metrics and how streams changed uptake rates as concentration increased (response slopes). In addition to altitude and temperature, other explanatory variables such as canopy cover, chlorophyll-**a** concentrations, transient storage size and exchange rates, and ambient DIN:SRP ratios were analyzed against uptake metrics and biological response. Models were considered statistically significant if p-values were < 0.05.

RESULTS

Elevation, Temperature, Canopy Cover, and Epilithon

Average stream temperatures recorded by the multi-parameter sonde over the duration of the nutrient slug addition varied from approximately 6-17 °C (Table 2, Figure 5a). Minimum temperatures logged on the iButtons during the 10 days prior to the experiment ranged from 4.5-15 °C between streams (Figure 5b). While the general trend of the elevation-temperature relationship was a decrease in temperature with an increase in elevation, there was a large influence from canopy cover on daytime temperatures. Channel shading by riparian tree cover was less frequent above 2900 m as the forest transitioned to alpine grassland (Table 3, Figure 6). Open canopy streams had daytime temperatures that were higher than expected for their elevation due to greater solar radiation throughout the day.

However, this “alpine effect” was not apparent in the 10-day minimum temperatures recovered from the iButtons (Figure 5b).

The deployed iButtons were not entirely successful, experiencing a number of failures that resulted in gaps in the long-term temperature data. For example, no iButton data could be retrieved from Caribou or West Fork Sheep Creek and only partial data was retrieved from loggers at Elkhorn, Izzy, and Wigwam Creeks. For the Elkhorn Creek, minimum, maximum, and average temperatures were derived from data available within 10 days prior to the date of the experiment and for Izzy and Wigwam Creeks temperatures were derived from the 10 days after the experiment.

Chlorophyll-**a** concentrations resulting from the epilithon sampling ranged from 0.01-1.02 mg m^{-2} across streams and did not predictably vary with altitude (Figure 7a) or temperature (Figure 7b)(Table 3). Contrary to expectations, percent canopy cover also did not have any detectable influence on epilithon chlorophyll-**a** standing stocks (Figure 7c).

HYDROLOGY

Because the 2011-2012 winter snowpack was abnormally low, most of the streams in this study had very low flow on the day of the nutrient addition compared to long-term averages. Two streams, Big Thompson and Trail Creek, went dry shortly after being the nutrient additions and have been omitted from this analysis. Stream discharges ranged from 3.5 to 120 L s^{-1} among streams, with ten varying between 20-70 L s^{-1} (Tables 4). Though there was no significant relationship

between discharge and elevation, streams with larger discharges tended to be warmer. The cross sectional area of the transient storage zone (A_S) ranged between 8-22% of the channel's cross-sectional area (A) and the exchange rate between the storage zone and the main channel (α) ranged from 0.4-9.5 x 10^{-3} s^{-1}. The exchange rates translate to mean channel residence times ranging from 1.7-43.7 minutes. The spatial ratio A_S/A is also equivalent to the ratio of exchange rates between each environment (channel and transient storage zone). Therefore, the mean residence time water stays in transient storage prior to reentering the channel ranged from 0.2-6.9 minutes. None of these hydrological parameters showed a relationship with altitude or temperature. A summary of the transient storage modeling is presented in Tables 4.

NUTRIENT DYNAMICS

Background Nutrient Conditions: Specific conductance was relatively low in all streams (22-45 μS cm^{-1}) with the exception of Elkhorn, which had a specific conductance of 155 μS cm^{-1} at the time of the addition. Ambient concentrations of both NH_4^+ and SRP were low in all streams, ranging from 1.5-8.8 μg-N L^{-1} and 0.6-10.1 μg-P L^{-1}, respectively. Nitrate was much more variable between streams ranging from 1.5-230.8 μg-N L^{-1}. Total dissolved inorganic nitrogen (DIN) ranged from 3.7-235.6 μg N L^{-1} (Table 5). Background concentrations of NH_4^+ and NO_3^- had significant, but opposite, relationship with elevation. While NH_4^+ concentrations decreased with increasing elevation ($p = 0.047$), NO_3^- concentrations increased with

elevation ($p = 0.014$). Background SRP concentrations also tended to decrease with elevation, but this trend was not significant ($p = 0.18$).

Nitrate was generally the dominant form of inorganic nitrogen, especially in streams with high DIN concentrations. This was not necessarily the case in streams with low DIN concentrations (< 1 μmol L^{-1}), where both NH_4^+ and NO_3^- contributed to the pool with similar relative quantities. The DIN:SRP molar ratios ranged between 1-76.2 in 14 of the 15 streams with Fall River as the exception with a DIN:SRP ratio of 544. All streams with a DIN:SRP ratio suggesting P limitation (> 16, based on the Redfield Ratio) exhibited cooler 10-day minimum temperatures (Figure 8) and were also cooler in general during the nutrient additions than those streams that had DIN:SRP ratios that suggested N limitation (< 16).

Ambient Metrics:

Regression: Performing regressions on S_w versus concentration plots was complicated by the different behaviors of the ascending and descending limbs of the breakthrough curves (Figure 9). To address this, three separate regressions were performed: one for each limb (reported here as ascending and descending) and one incorporating both limbs (reported here as the TASCC approach, sensu Covino et al. 2010), producing a range in ambient uptake metrics for each stream (Figures 10). The magnitude of variation in ambient uptake metrics was largely driven by hydrology, specifically the relative size of the storage zone (A_S/A), where more storage results in a larger range in uptake lengths and velocities (Figures 11).

Uptake lengths (S_w) were converted to uptake velocities (V_f) to normalize values to the variability between stream flow regimes. Ambient estimates of V_f for all three nutrients did not show significant interactions with altitude or any quantification of temperature or thermal regime (Figures 12). They also did not generally relate to the relative nutrient availability (DIN:SRP Molar Ratio), however V_f for the ascending limb of NH_4^+ did significantly decrease with increased relative nitrogen availability (p = 0.015, Figure 13).

Trends in areal uptake rates (U) versus altitude and temperature were the similar across all uptake calculation methods but the significance of those relationships varied. Areal uptake rates for NH_4^+ showed a significant negative relationship with altitude (Figure 14a), regardless of estimation method. Nitrate uptake rates had a positive relationship with altitude, but only the ascending rates were significantly correlated (p = 0.038)(Figure 14b). Similar to NH_4^+, SRP uptake rates decreased with an increase in altitude, however none of these relationships were significant (Figure 14c). TASCC areal uptake rates for NH_4^+, determined via regression, showed a significant positive relationship with temperature during the additions (p = 0.0032) while TASCC uptake rates for NO_3^- showed a curious negative trend with temperature (p = 0.14). TASCC uptake rates for SRP displayed a positive trend with temperature during the addition (slug temperature), however this relationship was not significant (p = 0.23). Ascending and descending uptake rates followed the same general trends as the TASCC uptake rates, the ascending uptake rates tended to be better predicted by slug temperature.

How temperature was quantified also had an effect on the significance of the relationship between temperature and uptake rates. Daytime minimums, maximums, and means were poor predictors for all nutrients. The 10-day maximums and means also tended to be poor predictors of uptake, but the long-term minimums showed strong correlations with NH_4^+ uptake, and were the best predictors of areal uptake rates for all nutrient forms (Figures 15). Ascending limb uptake rates of NH_4^+ were correlated strongest with the 10-day minimum temperatures.

Results from generalized linear models, simplified by backwards selection, were not different than the 2-way linear models for any uptake metric for all nutrient forms. After removing all insignificant terms, models contained only one significant explanatory variable (elevation, addition temperature, or quantification of thermal regime) and thus were effectively the same as the linear models.

Mass-Balance: A comparison of the areal uptake rate (U) estimations from the TASCC and mass balance calculation methods is shown in Figures 16, where a 1:1 line is included to show where both methods would have equal estimations. The mass balance approach tends to result in larger U values than does the average TASCC approach for NH_4^+ but U values for NO_3^- and SRP are roughly 1:1. Calculating uptake velocities and rates using the mass balance approach resulted in the same general trends as the TASCC regression approach. Uptake velocities were not found to be significantly affected by temperature or elevation for any of the nutrients, where the ascending uptake velocity (V_f) of NH_4^+ with 10-day minimum

temperatures had the strongest relationship (p = 0.097). However, when converted to areal uptake rate (U), there was a significant positive relationship with 10-day minimum temperatures and NH_4^+ (p = 0.0045), a modestly significant negative relationship for NO_3^- (p = 0.05), and no relationship with SRP (p = 0.62). Uptake rates calculated using the mass balance approach, much like the regression approach, showed a significant negative relationship with altitude and NH_4^+ uptake (p = 0.02) and a significant positive relationship with altitude and NO_3^- uptake (p = 0.03). Uptake rates of SRP did not exhibit any discernible trend with altitude.

Uptake Versus Concentration Relationships: Uptake rate versus concentration plots for all three nutrients did not appear to approach saturation, rather the relationship remained linear across concentrations for almost all nutrients at all sites (Figure 17a). Therefore, the slopes resulting from linear regressions (Figure 17b) were used to quantify biological response to increased nutrient availability instead of U_{max} and K_s values derived from fitting a Michaelis-Menten saturation function.

Response slopes did not vary systematically with elevation for any of the three nutrients added (NH_4^+, NO_3^-, and SRP), but NO_3^- response did increase significantly with the 10-day minimum temperatures (p = 0.017)(Figure 18a). Ammonium response also showed a positive relationship with the 10-day minimum temperature, however this trend was not significant (p = 0.081)(Figure 18b). No discernible pattern was found with SRP uptake response and temperature (Figure 18c).

DISCUSSION

The goal of this study was to compare streams across a natural altitude gradient in order to gain insight on how thermal regimes affect ambient rates of nutrient use and the rate of biological response to increased nutrient supply. This study also implemented a recently developed approach to nutrient additions, leading to an opportunity to assess the method. I found that ambient uptake rates of NH_4^+ varied systematically with both the altitude and temperature gradient and, surprisingly, that the response of NO_3- uptake increased with long-term minimum temperatures.

AMBIENT METRICS

TASCC Estimations: Ambient uptake lengths were estimated for each stream by fitting a linear regression through a plot of each sample's individual uptake length versus its respective concentration and extrapolating to background conditions as per Payn et al. (2005). However, this process was complicated by the differing trends associated with the ascending and descending limbs of the breakthrough curves (Figure 9). In most cases, the limbs acted seemingly independent of each other, yielding radically different estimates of uptake length, and thus areal uptake rate, for a given stream depending on which data points are included in the regression (Figures 10).

The differing trends of ascending and descending limbs are not likely to be analytical artifacts but rather are true reflections of stream ecosystem behavior. There is no evidence in the chemical analyses to suggest that there is sufficient error

to explain the differential patterns observed in ascending and descending portions of the observed BTCs. Historically, nutrient uptake in streams was derived from constant rate injections in which solutes were added to the stream at a known rate until concentrations stabilized through the entire study reach. Sampling of the conservative and reactive tracer at several longitudinal locations was used to estimate k_L, S_W, and other metrics using the expressions presented earlier. Under plateau conditions, water samples reflect the summed influence of all flow paths active in the experimental reach. Consequently, differential biological processing rates associated with rapid, intermediate, and slow paths are proportionately represented in the chemistry of each water sample. However, by assessing uptake under a single enrichment level it is impossible to examine the dependency of uptake on nutrient concentration and therefore have confidence that the uptake metrics that result from this approach match ambient uptake characteristics (Mulholland et al. 2000, Dodds et al. 2002, Payn et al. 2005, Earl et al. 2006, O'Brien and Dodds 2010). The Tracer Approach to Spiraling Curve Characterization (TASCC) was designed to examine the dynamic response of a stream to changing nutrient concentrations by examining the behavior of conservative and reactive solutes as concentration rise and fall through the downstream BTC and thus quantify the relationship between nutrient enrichment and spiraling metrics (Covino e al. 2010a). However, tracer concentrations associated with water samples collected during the course of the BTC are not representative of the full range of stream flowpaths but rather reflect the specific conditions experienced along flowpaths with specific residence times. Samples collected earlier in the

breakthrough curve, during the ascending limb, experienced faster average flow velocities (by definition) and reflect activity in the advective channel whereas water parcels collected on the descending limb incorporate activity associated with slow-moving pools of water or porous material in the streambed or bank referred to as transient storage zones (and estimated by the OTIS model, Runkel 1998).

The ability for solutes to interact to with the biology or a sorptive-surface differs greatly by flow path. Generally, the benthos is the portion of a stream with the most biological activity. By comparison, planktonic activity is often negligible in small, turbulent streams (Vannote et al. 1980). In contrast, biogeochemical activity in hyporheic environments varies with rate of hydrological fluxes and the distribution of redox conditions. In general, aerobic metabolism in the hyporheic tends to be similar or slower than benthic rates, though unique anaerobic processes may be active. Slower aerobic metabolism in the hyporheic could lead to an underestimation of uptake in the main channel when the higher solute concentrations of transient storage water mask the removal of that solute from the main channel as they continue to exchange water. Combined, it is unsurprising to observe drastically different trends emerge from the two limbs of the breakthrough curve. It should be noted, however, that regressions through the ascending limbs did not always exhibit the more rapid uptake rate (shorter uptake length) relative to the descending limbs.

In the original presentation of the TASCC method, Covino et al (2010a) did not report differential behavior in the relationship between S_w and added concentration on the rising and falling limb of their BTCs and therefore did not

explore the mechanisms responsible for such differences (or lack thereof). Covino et al (1010a) did explore two different approaches for estimating V_f and U: (1) using a variable travel rate, where each sample is matched with its specific mean velocity based on sampling time, and (2) use of constant travel rate based on the mean velocity derived from the time-to-peak of the breakthrough curve. In that application, using variable travel times (as conducted in this analysis) resulted in a hysteresis in the uptake versus added concentration relationship in which then rising limb had higher uptake rates relative to the falling limb (clockwise hysteresis). When uptake rates (U) were calculated using a constant travel time the hysteresis was lost. They suggested that the hysteretic behavior in V_f and U curves calculated using variable travel times was an artifact of the calculation method since the hysteresis was not apparent in the plots for S_w, a time-independent metric. Data from this study disputes their conclusion of forced hysteresis by the inclusion of variable travel times, as S_w lengths versus concentration trends from the opposing limbs of the breakthrough curve were not similar in behavior. In this research we observed situations in which using the actual travel time both exaggerated or reduced hysteric relationships between uptake rates and concentration (U vs. C) suggesting that using a constant travel time does not always eliminate such effects.

So what is the most appropriate way to quantify spiraling metrics using data from slug additions of reactive solutes? In this study, uptake metrics were calculated using a variety of approaches. Following the TASCC approach (Covino et al. 2010a), S_w versus concentration regressions were performed on plots containing all individual uptake lengths from a given stream and were reported as the TASCC

rates. Separate regressions were also performed on data explicit to either the ascending or descending limbs of the breakthrough curve, reported as ascending and descending rates, respectively. I also used a mass balance approach in which BTC were integrated to estimate the total mass lost as the slug traveled through each experimental reach and used that loss to estimate a single set of uptake metrics. Uptake rates estimated by the mass balance approach generally exceeded ambient rates calculated by the TASCC approach (derived from a single S_W vs. C regression). This result is most likely due to the nutrient enrichment effect that isn't accounted for in the mass balance approach. Uptake rates from both the ascending and descending limbs bracketed estimates of those produced by the TASCC (by definition) and mass balance methods. Combining estimates of ambient uptake metrics based on all points and those just associated with the rising and falling limbs effectively produces estimates of the maximum, minimum and average behavior of the stream under ambient conditions condition for a stream and provides a more comprehensive understanding of nutrient uptake in streams by defining a range of processing rates and how they differ between rapid and slow flowpaths.

Various researchers have explored the biogeochemical activity of transient storage zones and their contribution to overall nutrient retention in stream ecosystems (Mulholland et al. 1997, Valett et al. 1997, Thomas et al. 2003, Runkel 2007, Baker et al. 2012). Findings from this study, where ascending and descending limbs of the breakthrough curve exhibited their own distinct behavior in removal rates, further support a transition toward quantifying nutrient uptake and retention

in a manner that includes the inherent heterogeneity in reactivity among microhabitats within a given stream. Thus, I argue that uptake should not be reported as a single value for one stream, but rather as a range of rates that define the variation of nutrient cycling in streams.

Since a comprehensive method for incorporating all the aspects of a stream's heterogeneity has not yet been created, much of the focus of this study was on the uptake dynamics of the ascending limb from the BTC. Uptake metrics for the ascending limb tended to be the most describable with my dataset, where the long-term minimum temperatures were the best descriptor of any uptake metric for each nutrient. Thus, attention is primarily on areal uptake rates and velocities versus 10-day minimum stream temperatures.

Uptake Rates and Temperature: Uptake rates for both NH_4^+ and SRP showed a positive relationship with temperature, as predicted in our hypothesis, while NO_3^- had a negative relationship with temperature. These trends were consistent across all methods for estimating uptake rate and all quantifications of thermal regime, but the strength of these relationships varied by calculation method and nutrient.

Ammonium uptake rates, regardless of estimation method, were found to be significantly related to the average temperature during the addition and to minimum temperatures on the day of the experiment or from an adjacent 10-day period. No such relationship was observed with maximum temperatures suggesting that minimum temperatures may act as a bottleneck constraining the activity or standing stocks of microbial communities in these streams. Poor correlation

between periphyton standing stocks and ambient NH_4^+ metrics support the conclusion that biomass-specific activity rather than standing stocks may be responsible for the observed differences in these streams.

Nitrate areal uptake rates consistently showed a negative relationship with temperature, though none of the relationships were found to be significant. Valett et al. (2008) reported inverse relationships of NO_3^- uptake rates with temperature in closed canopy systems when assessed across seasons, but this was primarily driven by high standing stocks of leaves in streams during the fall and algal activity in the winter prior to leaf-out. One potential explanation for the inverted relationship, relative to our hypothesis, is the possibility of increased rates of nitrification with increasing temperatures. This is unlikely, however, because uptake rates of NO_3^- were much greater than NH_4^+, in many instances by an order of magnitude, suggesting that the potentially increased rates of conversion of NH_4^+ to NO_3^- at higher temperatures would not be enough to explain the negative trend. Another possible explanation for the opposing trends of NH_4^+ and NO_3^- uptake with temperature could be from the relative diffusion rates across the laminar surface of an organism's cells. Diffusion rates are driven primarily by concentration gradients, where cells reduce the concentration of a nutrient within relative to their environment, allowing for passive transport across the cell membrane. The streams exhibiting lower temperatures in this study tended to have relatively higher ambient concentrations of NO_3^- and lower concentrations of NH_4^+, thus the concentration gradient across the laminar surface would be greater for NO_3^- than NH_4^+, resulting in quicker rates of diffusion of NO_3^- into each cell compared to NH_4^+.

In this scenario, the streams with lower temperatures (and higher NO_3^-) concentrations would be obtaining a larger percentage of their N demand from NO_3^- instead of NH_4^+.

It is also possible that the biological community present at the streams with higher NO_3^- concentrations were "primed" to more efficiently take up NO_3^- than other streams. Given that high nitrate streams tended to occur at high elevations, likely due to atmospheric deposition of N and snowpack being greater at higher elevations (Stottlemyer et al. 1997, Mladenov et al. 2012), the negative relationship between ambient NO_3^- and temperature is likely to be a spurious artifact of the patterns in ambient nutrient concentrations. How those gradients effect NH_4^+ uptake is less clear but the different relationships between temperature and ammonium U and V_f suggest that trends in ambient NH_4^+concentration reinforce the relationship between temperature and NH_4^+ uptake rates observed in this study.

The relationship between ambient SRP uptake and temperature was not found to be significant for any uptake estimate or quantification of temperature or thermal regime. This suggests that thermal variation among streams is not the primary driver of SRP uptake, possibly due to the tendency of ortho-phosphate (PO_4^{3-}) to abiotically sorb to many substrates (Lottig and Stanley 2007). The temporary sorption of SRP to substrates in the benthos and/or the transient storage zone could result in an overestimation of uptake in quicker flowpaths since some of the SRP loss from the water column would not be due to biological processes. Moreover, the eventual release of SRP from the sorptive surface back to the water column would cause an underestimation of uptake on samples gathered from

slower flowpaths as much of the measured SRP could be an artifact of desorption, masking biological uptake.

Ambient Concentrations and Uptake Efficiencies: Background concentrations of both NH_4^+ and NO_3^- varied systematically along the altitude gradient, where NH_4^+ concentrations decreased with increasing altitude and NO_3^- concentrations increased with altitude, potentially due to increased rates of in-stream nitrification or atmospheric NO_3^- deposition at higher altitudes. Background SRP concentrations showed a pattern with elevation similar to that observed for NH_4^+, but the relationship was not significant. The systematic variation of ambient nutrient concentrations across our altitude gradient was not expected and these values were unknown at the time of the experiment. The unintended relationship between altitude, and consequently temperature, and background nutrient concentrations complicates my assessment of the relationship between altitude (or temperature) and uptake rate because background concentration is used in the calculation (U = (Q * $\boldsymbol{C}$) / (S_W* w)). As a result, it's difficult to tease apart whether temperature is driving changes in uptake rate or whether its nutrient concentration. Uptake rates are commonly used in preference to V_f and S_w to compare many streams because it's the most direct reflection of nutrient use by the biological community (how much nutrient is taken up by a specific areas of stream bed per unit time). Ironically, in this situation it creates an autocorrelation between dependent and explanatory variables, where variation of U with altitude or temperature could be an artifact of ambient nutrient concentrations.

The assumption that the systematic variation in ambient conditions along the altitude gradient influenced the relationship of *U* with temperature and altitude is further supported by examining patterns of variation in V_f. Uptake velocities for all nutrients, regardless of estimation approach, did not exhibit a significant relationship with temperature or altitude. Moreover, ascending V_f for NH_4^+ had a significant negative relationship with molar DIN:SRP (Fall Creek omitted for being outlier), where increased relative nitrogen availability reduced the theoretical rate which an NH_4^+ molecule approaches its point of uptake. This relationship of V_f with DIN:SRP did not hold true with NO_3^- or SRP and could be why *U* for these nutrients did not significantly trend with temperature.

Uptake Responses to Nutrient Loading

M-M Kinetics: Nutrient releases in this study were designed to; (a) alleviate any potential constraints posed by limited nutrient availability by adding all three nutrients simultaneously, and (b) deliver sufficient nutrient loads to examine how uptake metrics change with increasing nutrient availability. However, uptake versus concentration plots did not reveal saturating conditions and responses were fairly linear among nutrients across all sites even though concentrations were at or above saturating levels reported in other studies (Covino et al. 2010a, 2010b). Therefore, the Michaelis-Menten model could not be fit to *U* vs. *C* curves with any certainty in the magnitude of its descriptive parameters.

There are several reasons why this study failed to reach saturating conditions. One potential explanation could be the addition of all nutrients

simultaneously. We chose to release solutes all at once to ensure the uptake of one nutrient was not constrained by another, helping isolate the influence of temperature on assimilation. However, by allowing essentially unlimited nutrient resources, the biota could have responded with increased rates of luxury uptake, where organisms were stripping nutrients from the water column while not immediately incorporating the N or P in to their biomass. Schade et al. (2011) found that autotrophic streams can exhibit plasticity in stoichiometric uptake rates ($U_{N:P}$) upon changes in relative nutrient supplies. This argument for lack of saturation is supported by molar DIN:SRP uptake ratios of less than 9:1 across all streams, well below the Redfield Ratio of 16:1, suggesting that more P was being taken up than can be immediately incorporated in to biomass or that there was a large abiotic role in P removal, such as sorption to sediments.

Another possible reason for not approaching saturated conditions could be due to adding nutrients as a slug rather than using a constant rate injection. When nutrients are released as a single slug, or pulse, each theoretical flow path experiences only a limited range of concentrations for a very brief period of time instead of the entire stream being subjected to heavy nutrient loads for an extended duration. This could result in the biology not having time to respond "properly" to the extreme conditions, potentially leading to increased luxury uptake as noted prior.

Pulse additions could also be an inappropriate method for addressing uptake kinetics because each sample represents the biological function of only that specific flow path. Comparing the function of the distinct microhabitats within each flow

path as though they were homogenous across the entirety of the stream poses some potential issues. Transient storage zones do not necessarily have the same uptake potential as the main channel (Runkel 2007) and while reaction time was accounted for between streams by the targeted 15-minute residence time, each sample collected for a given stream had an inherently different time of exposure to a reactive substrate. These issues combined could confound the ability to treat all *U* versus *C* points acquired from a single injection to describe the stream's ability as a whole to respond to increased nutrient loads.

Linear Response Slopes: Biological response to availability was quantified by fitting *U* vs. *C* plots with a linear regression instead of using a Michaelis-Menten framework, where the magnitude of the linear regression's slope is the sole descriptor of response in uptake to increased nutrient availability. Response slopes for NH_4^+ and SRP did not display a significant trend with altitude or any quantification of temperature. Ammonium response with temperature was strong, but not significant, likely due to the large gap in the temperature gradient. Nitrate response did have a significant relationship with 10-day minimum temperatures, however this is largely due to the leverage of a single data point on the far end (highest temperature) of the temperature gradient. The lack of streams exhibiting minimum thermal regimes from about 10-15 °C in this study created an un-ideal scenario, where the warmest stream determined whether trends were significant much of the time.

Conclusions

The initial findings of long-term thermal minimums driving uptake rates were confounded by ambient nutrient concentrations varying systematically with the altitude gradient and an insufficient representation of the thermal gradient, where few streams exhibited warm temperatures. Uptake velocities failed to exhibit the same significant trends, implying that the aforementioned relationships could be an artifact of calculation methods. Responses of uptake rates of stream biota to increased nutrient availability produced a significant relationship with 10-day minimum temperatures for NO_3^-, but not for NH_4^+ or SRP, though the relationship with NH_4^+ and minimum temperature was strong.

Marti et al. (2009) was also unable to reveal temperature as a driver of nutrient uptake among streams and used a similar approach to "manipulating" thermal regime as this study, by sampling streams across an altitude gradient. Because temperature gradients were created indirectly by strategically sampling at varying altitudes, it is possible that the stream biota has sufficiently adapted to local thermal regimes to the extent that a given stream's absolute temperature is not a good predictor of uptake but rather the departure from normal temperatures being the driver of uptake rates. This study did not directly manipulate in-stream temperatures, however, so that conclusion cannot be confirmed. Based on these results, future studies regarding how stream temperature affects ambient nutrient uptake rates and uptake kinetics should manipulate temperature in a more direct manner, avoiding natural temperature gradients where local adaptation, among many other factors, could mask the relationship.

LITERATURE CITED

Baker, D.W., Bledsoe, B.P., Price, J.M. 2012. Stream nitrate uptake and transient storage over a gradient of geomorphic complexity, north-central Colorado, USA. Hydrological Processes 26(21):3241-3252.

Bencala, K.E. and Walters, R.A. 1983. Simulation of solute transport in a mountain pool-and-riffle stream – a transient storage model. Water Resources Research 19(3):718-724.

Bernot, M.J., Martin, E.C., Bernot, R.J. 2010. The influence of trophic complexity on preferential uptake of dissolved inorganic and organic nitrogen: a laboratory microcosm experiment. Journal of the North American Benthological Society 29(4)1199-1211.

Bott, T.L. and Newbold, J.D. 2013. Ecosystem metabolism and nutrient uptake in Peruvian headwater streams. International Review of Hydrobiology 98(3):117-131.

Boulton, A.J. 1993. Stream ecology and surface hyporheic hydrologic exchange – implications, techniques and limitations. Australian Journal of Marine and Freshwater Research 44(4):553-564.

Cardenas, M.B. and Wilson, J.L. 2007. Effects of current-bed form induced fluid flow on the thermal regime of sediments. Water Resources Research. 43:W08431

Covino, T.P., McGlynn, B.L., McNamara, R.A. 2010a. Tracer Additions for Spiraling Curve Characterization (TASCC): Quantifying stream nutrient uptake kinetics from ambient to saturation. Limnology and Oceanography-Methods 8:484-498.

Covino, T.P, McGlynn, B.L., Baker, M.A. 2010b. Separating physical and biological nutrient retention and quantifying uptake kinetics from ambient to saturation in successive mountain stream reaches. Journal of Geophysical Research 115:G04010.

Dodds, W.K., Lopez, A.J., Bowden, W.B., Gregory, S., Grimm, N.B., Hailton, S.K., Hershey, A.E., Marti, E., McDowell, W.H., Meyer, J.L., Morrall, D., Mulholland, P.J., Peterson, B.J., Tank, J.L., Valett, H.M., Webster, J.R., Wollheim, W. 2002. N uptake as a function of concentration in streams. Journal of the North American Benthological Society 21(2):206-220.

Earl, S.A., Valett, H.M., and Webster, J.R. 2006. Nitrogen saturation in stream ecosystems. Ecology 87(12):3140-3151.

Hall, R.O., Tank, J.L., Sobota, D.J., Mulholand, P.J., O'Brien, J.M., Dodds, W.K., Webster, J.R., Valett, H.M., Poole, G.C., Peterson, B.J., Meyer, J.L., McDowell, W.H., Johnson, S.L., Hamilton, S.K., Grimm, N.B., Gregory, S.V., Dahm, C.N., Cooper, L.W., Ashkenas, L.R., Thomas, S.M., Sheilbley, R.W., Potter, J.D., Niederlehner, B.R., Johnson, L.T., Helton, A.M., Creshaw, C.M., Burgin, A.J., Bernot, M.J., Beaulieu, J.J., Arango, C.P. 2009. Nitrate removal in stream ecosystems measured by N-15 addition experiments: Total uptake. Limnology and Oceanography 54(3):653-665.

Holmes, R.M., Aminot, A., Kerouel, R., Hooker, B.A., Peterson, B.J. 1999. A simple and precise method for measuring ammonium in marine and freshwater ecosystems. Canadian Journal of Fisheries and Aquatic Sciences 56:1801-1808.

IPCC, 2007: Climate Change 2007: The Physical Science Basis. Contibution of Working Group I to the Fourth Assessment Report of the Intergovernmental Panel on Climate Change [Solomon, S., D. Qin, M. Manning, Z. Chen, M. Marquis, K.B. Averyt, M. Tignor and H.L. Miller (eds.)]. Cambridge University Press, Cambridge, United Kingdom and New York, NY, USA.

Kim, B.K., Jackman, A.P., and Triska, F.J. 1990. Modeling transient storage and nitrate uptake kinetics in a flume containing a natural periphyton community. Water Resources Research 26(3):505-515.

Kim, B.K., Jackman, A.P., Triska, F.J. 1992. Modeling biotic uptake by periphyton and transient hyporheic storage of nitrate in a natural stream. Water Resources Research 28(10):2743-2752.

Lottig, N.R. and Stanley, E.H. 2007. Benthic sediment influence on dissolved phosphorous concentrations in a headwater stream. Biogeochemistry 84(297-309.

Marti, E., Fonolla, P., von Schiller, D., Sabater, F., Argerich, A., Ribot, M., and Riera, J. 2009. Variation in stream C, N, and P uptake along an altitudinal gradient: a space-for-time analogue to assess potential impacts of climate change. Hydrology Research 40(2):123-137.

Mladenov, N., Williams, M.W., Schmidt, S.K., Cawley, K. 2012. Atmospheric deposition as a source of carbon and nutrients to an alpine catchment of the Colorado Rocky Mountains. Biogeosciences 9(8):3337-3355.

Mulholland, P.J., Marzolf, E.R., Webster, J.R., Hart, D.R., Hendricks, S.P. 1997. Evidence that hyporheic zones increase heterotrophic metabolism and

phosphorous uptake in forest streams. Limnology and Oceanography 42(3):443-451.

Mulholland, P.J., Tank, J.L., Sanzone, D.M., Wollheim, W.M., Peterson, B.J., Webster, J.R., Meyer, J.L. 2000. Nitrogen cycling in a forest stream determined by a N-15 tracer addition. Ecological Monographs 70(3):471-493.

Mulholland, P.J., Thomas, S.A., Valett, H.M., Webster, J.R., Beaulieu, J. 2006. Effects of light on NO3- uptake in small forested streams: diurnal and day-to-day variations. Journal of the North American Benthological Society 25(3):583-595.

Mulholland, P.J., Helton, A.M., Poole, G.C., Hall Jr., R.O., Hamilton, S.K., Peterson, B.J., Tank, J.L., Ashkenas, L.R., Cooper, L.W., Dahm, C.N., Dodds, W.K., Findlay, S.E.G., Gregory, S.V., Grimm, N.B., Johnson, S.L., McDowell, W.H., Meyer, J.L., Valett, H.M., Webster, J.R., Arango, C.P., Beaulieu, J.J., Bernot, M.J., Burgin, A.J., Crenshaw, C.L., Johnson, L.T., Niederlehner, B.R., O'Brien, J.M., Potter, J.D., Sheibley, R.W., Sobota, D.J., Thomas, S.M. 2008. Stream denitrification across biomes and its response to anthropogenic nitrate loading. Nature 452:202-205.

Murphy, J. and Riley, J.P. 1962. A modified single solution method for the determination of phosphate in natural waters. Analytic Chimica Acta 27:31-36.

Newbold, J.D., Elwood, J.W., O'Neill, R.V., Van Winkle, W. 1981. Measuring nutrient spiraling in streams. Can. J. Fish. Aquat. Sci. 38:860-863.

Newbold, J.D., Mulholland, P.J., Elwood, J.W., O'Neill, R.V. 1982a. Organic carbon spiraling in stream ecosystems. OIKOS 38:266-272.

Newbold, J.D., O'Neill, R.V., Elwood, J.W., Van Winkle, W. 1982b. Nutrient spiraling in streams: implications for nutrient limitation and invertebrate activity. The American Naturalist 120(5):628-652.

Newbold, J.D., Elwood, J.W., O'Neill, R.V., Sheldon, A.L. 1983. Phosphorous dynamics in a woodland stream ecosystem: a study of nutrient spiraling. Ecology 64(5):1249-1265.

Newbold, J.D. 1992. Cycles and Spirals of Nutrients. In: The Rivers Handbook (eds P. Calow and G.E. Petts) pp. 379-408. Blackwell Science, Oxford.

O'Brien, J.M. and Dodds, W.K. 2010. Saturation of NO3- uptake in prairie streams as a function of acute and chronic N exposure. Journal of the North American Benthological Society 29(2):627-635.

Payn, R.A., Webster, J.R., Mulholland, P.J., Valett, H.M., Dodds, W.K. 2005. Estimation of stream nutrient uptake from nutrient addition experiments. Limnology and Oceanography-Methods 3:174-182.

Runkel, R.L. 1998. One-dimensional transport with inflow and storage (OTIS): A solute transport model for streams and rivers. Water-Resources Investigations Report 98-4018.

Runkel, R.L. 2007. Towards a transport-based analysis of nutrient spiraling and uptake in streams. Limnology and Oceanography-Methods. 5:50-62.

Schade, J.D., MacNeill, K.L., Thomas, S.A., McNeely, F.C., Welter, J.R., Hood, J., Goodrich, M., Power, M.E., Finlay, J.C. 2011. The stoichiometry of nitrogen and

phosphorous spiraling in heterotrophic and autotrophic streams. Freshwater Biology 56(3):424-436.

Stottlemyer, R., Troendle, C.A., Markowitz, D. 1997. Change in snowpack, soil watere, and streamwater chemistry with elevation during 1990, Fraser Experimental Forest, Colorado. Journal of Hydrology 195(1-4):114-136.

Stream Solutes Workshop 1990. Concepts and methods for assessing solute dynamics in stream ecosystems. J. N. Am. Benthol. Soc. 9(2):95-119.

Tank, J.L., Meyer, J.L., Sanzone, D.M., Mulholland, P.J., Webster, J.R., Peterson, B.J., Wollheim, W.M., Leonard, N.E. 2000. Analysis of nitrogen cycling in a forest stream during autumn using a N-15-tracer addition. Limnology and Oceonography 45(5):1013-1029.

Tank, J.L., Rosi-Marshall, E.J., Baker, M.A., Hall Jr., R.O. 2008. Are rivers just big streams? A pulse method to quantify nitrogen demand in a large river. Ecology 89(10):2935-2945.

Taylor, B.W., Keep, C.F., Hall Jr., R.O., Koch, B.J., Tronstad, L.M., Flecker, A.S., Ulseth, A.J. 2007. Improving the fluorometric ammonium method: matrix effects, background fluorescence, and standard additions. Journal of the North American Benthological Society 26:167-177.

Thomas, S.A., Valett, H.M., Webster, J.R., Mulholland, P.J. 2003. A regression approach to estimating reactive solute uptake in advective and transient storage zones of stream ecosystems. Advances in Water Resources 26(9):965-976.

Triska, F.J., Kennedy, V.C., Avanzino, R.J., Zellweger, G.W., Bencala, K.E. 1989. Retention and transport of nutrients in a third-order stream: channel processes. Ecology 70(6):1877-1892.

Valett, H.M., Dahm, C.N., Campana, M.E., Morrice, J.A., Baker, M.A., Fellows, C.S. 1997. Hydrological influences on groundwater surface water ecotones: Heterogeneity in nutrient composition and retention. Journal of the North American Benthological Society 16(1):239-247.

Valett, H.M., Thomas, S.A., Mulholland, P.J., Webster, J.R., Dahm, C.N., Fellows, C.S., Crenshaw, C.L., Peterson, C.G. 2008. Endogenous and exogenous control of ecosystem function: N cycling in headwater streams. Ecology 89(12):3515-3527.

Vannote, R.L., Minshall, G.W., Cummins, K.W., Sedell, J.R., Cushing, C.E. 1980. The river continuum concept. Canadian Journal of Fisheries and Aquatic Sciences 37:130-137.

von Schiller, D., Marti, E., Riera, J., Ribot, J., Argerich, A., Fonolla, P., Sabater, F. 2008. Inter-annual, annual, and seasonal variation of P and N retention in a perennial and intermitten stream. Ecosystems 11:670-687.

Webster, J.R. 1975. Analysis of potassium and calcium dynamics in stream ecosystems on three southern Appalachian watersheds of contrasting vegetation. Doctoral dissertation, Univ. Georgia, Athens, GA, USA. 232 p.

Webster, J.R. and Patten, B.C. 1979. Effects of watershed perturbation on stream potassium and calcium dynamics. Ecological Monographs 49(1):51-72.

Webster, J.R., Mulholland, P.J., Tank, J.L., Valett, H.M., Dodds, W.K., Peterson, B.J., Bowden, W.B., Dahm, C.N., Findlay, S., Gregory, S.V., Grimm, N.B., Hamilton, S.K., Johnson, S.L., Marti, E., McDowell, W.H., Meyer, J.L., Morrall, D.D., Thomas, S.A., Wollheim, W.M. 2003. Factors affecting ammonium uptake in streams – an inter-biome perspective. Freshwater Biology 48(8):1329-1352.

TABLES AND FIGURES

Table 1. Summary of study streams with their respective drainage, altitude, and coordinates.

Site	Basin	Altitude	Coordinates	
		m	Latitude	Longitude
Rock	St. Vrain	2643	40° 10' 21.847" N	105° 31' 40.409" W
Beaver	St. Vrain	2830	40° 7' 2.432" N	105° 31' 56.609" W
Caribou	St. Vrain	2964	39° 59' 45.402" N	105° 34' 4.552" W
Wigwam	St. Vrain	3249	40° 4' 14.596" N	105° 36' 12.028" W
Izzy	St. Vrain	3348	40° 4' 15.317" N	105° 36' 53.661" W
Miller Fork	Big Thompson	2252	40° 28' 47.781" N	105° 26' 41.454" W
Black Canyon	Big Thompson	2411	40° 24' 20.285" N	105° 32' 56.649" W
Hidden Valley	Big Thompson	2900	40° 23' 33.382" N	105° 39' 34.743" W
Big Thompson	Big Thompson	3365	40° 25' 32.111" N	105° 47' 2.526" W
Fall	Big Thompson	3478	40° 26' 16.689" N	105° 45' 12.769" W
Elkhorn	Cache la Poudre	1992	40° 41' 59.877" N	105° 26' 29.368" W
Trail	Cache la Poudre	2190	40° 55' 6.716" N	105° 29' 54.204" W
SPAM Pennock	Cache la Poudre	2775	40° 32' 57.298" N	105° 33' 42.022" W
Corral	Cache la Poudre	3060	40° 31' 5.186" N	105° 46' 14.769" W
West Fork Sheep	Cache la Poudre	3200	40° 36' 28.238" N	105° 43' 29.766" W

Table 2. Summary of temperatures and thermal regimes, in °C.

Site	Slug Temp	Day Mean	Day Min	Day Max	10-Day Mean	10-Day Min	10-Day Max
Black Canyon	11.2	11.0	10.0	12.5	10.8	8.5	12.5
Beaver	12.1	11.0	8.0	14.0	12.2	7.0	18.5
Caribou	11.2	n.a.	n.a.	n.a.	n.a.	n.a.	n.a.
Corral	13.7	13.5	10.5	16.0	13.2	8.5	17.5
Elkhorn	16.8	n.a.	n.a.	n.a.	16.7	15.0	20.0
Fall	7.3	10.8	8.0	14.5	11.5	4.5	21.5
Hidden Valley	6.2	5.8	5.0	6.5	5.8	4.5	8.0
Izzy	10.6	11.6	10.5	12.5	10.2	5.5	15.0
Miller Fork	13.6	13.2	9.5	15.5	13.9	9.0	20.5
Rock	8.0	8.1	7.0	9.5	8.3	7.0	10.5
SPAM Pennock	8.2	7.9	7.0	8.5	8.1	6.5	9.5
West Fork Sheep	9.8	n.a.	n.a.	n.a.	n.a.	n.a.	n.a.
Wigwam	9.4	7.4	6.0	9.0	7.6	5.5	10.0

Table 3. Summary of % canopy cover and chlorophyll-**a** concentrations with their respective stream, altitude, and temperature.

Site	Altitude	Slug Temp	10-Day Min	Canopy Cover	Chlorophyll-a
	(m)	(°C)	(°C)	%	mg m^{-2}
Beaver	2830	12.1	7.0	64.4	0.36
Black Canyon	2411	11.2	8.5	79.7	0.22
Caribou	2964	11.2	n.a.	1.3	0.19
Corral	3060	13.7	8.5	27.8	0.81
Elkhorn	1992	16.8	15.0	61.0	0.06
Fall	3478	7.3	4.5	0.0	0.15
Hidden Valley	2900	6.2	4.5	55.3	0.08
Izzy	3348	10.6	5.5	18.0	0.33
Miller Fork	2252	13.6	9.0	82.9	0.36
Rock	2643	8.0	7.0	79.5	0.23
SPAM Pennock	2775	8.2	6.5	69.7	0.01
West Fork Sheep	3200	9.8	n.a.	n.a.	n.a.
Wigwam	3249	9.4	5.5	58.7	1.02

Table 4a. Description of estimated hydrological parameters.

Variable	Description	Units
Q	Discharge	$L\ s^{-1}$
v	Mean Velocity	$m\ s^{-1}$
L	Reach Length	m
w	Stream Width	m
z	Stream Depth	m
D	Dispersion	$m^2\ s^{-1}$
A	Cross-Sectional Area	m^2
A_S	Storage Area	m^2
A_S/A	Relative Storage Area	n.a.
α	Exchange Rate	s^{-1}
k_w	Turnover Time (Main Channel)	min
TT	Turnover Time (Transient Storage Zone)	min

Table 4b. Summary of hydrological parameters.

Site	Q	v	L	w	z	D	A	A_s	A_s/A	α	k_w	TT
Beaver	118.1	0.22	347	3.87	0.14	0.44	0.49	0.048	0.10	9.54E-03	1.7	0.2
Big Thompson	2.9	0.06	66	1.26	0.04	n.a.	n.a.	n.a.	n.a.	n.a.	n.a.	n.a.
Black Canyon	32.1	0.18	234	1.93	0.09	0.32	0.17	0.018	0.11	1.13E-03	14.7	1.6
Caribou	67.5	0.25	195	2.09	0.13	0.26	0.23	0.043	0.19	3.46E-03	4.8	0.9
Corral	58.4	0.14	187	2.99	0.14	0.24	0.39	0.041	0.10	6.65E-04	25.1	2.6
Elkhorn	67.3	0.21	213	3.47	0.09	0.23	0.28	0.054	0.19	2.67E-03	6.2	1.2
Fall	3.6	0.11	76	0.53	0.06	n.a.	n.a.	n.a.	n.a.	n.a.	n.a.	n.a.
Hidden Valley	30.8	0.14	168	2.08	0.10	0.27	0.21	0.034	0.16	3.81E-04	43.7	6.9
Izzy	47.8	0.19	209	2.34	0.11	0.25	0.23	0.029	0.13	9.30E-04	17.9	2.3
Miller Fork	22.5	0.12	185	2.38	0.08	0.13	0.17	0.021	0.13	1.34E-03	12.4	1.6
Rock	34.8	0.22	222	1.71	0.09	0.40	0.15	0.015	0.10	7.74E-04	21.5	2.2
SPAM Pennock	20.3	0.10	142	1.86	0.10	0.15	0.19	0.017	0.09	5.03E-04	33.1	3.0
Trail	11.4	0.08	117	2.50	0.05	0.06	0.13	0.026	0.20	8.92E-04	18.7	3.7
West Fork Sheep	26.2	0.21	312	1.86	0.07	0.41	0.12	0.010	0.08	3.91E-04	42.7	3.3
Wigwam	7.1	0.07	90	1.61	0.06	0.04	0.09	0.020	0.22	1.88E-03	8.9	1.9

Table 5. Summary of ambient chemical conditions.

Site	SpC	NH_4^+		NO_3^-		DIN		SRP		N:P
		µg-N L^{-1}	µmol L^{-1}	µg-N L^{-1}	µmol L^{-1}	µg-N L^{-1}	µmol L^{-1}	µg-P L^{-1}	µmol L^{-1}	
Beaver	35	4.1	0.29	6.1	0.43	10.1	0.72	2.8	0.09	7.98
Black Canyon	38	7.9	0.56	1.5	0.11	9.4	0.67	8.5	0.27	2.45
Caribou	43	3.5	0.25	24.4	1.74	28.0	2.00	4.9	0.16	12.64
Corral	28	1.8	0.12	2.0	0.14	3.7	0.26	8.0	0.26	1.03
Elkhorn	155	8.8	0.63	4.4	0.32	13.3	0.95	8.3	0.27	3.54
Fall	45	1.6	0.11	148.6	10.61	150.2	10.72	0.6	0.02	544.16
Hidden Valley	24	1.6	0.11	78.3	5.59	79.9	5.71	10.1	0.33	17.46
Izzy	26	4.8	0.34	230.8	16.47	235.6	16.82	8.9	0.29	58.78
Miller Fork	44	3.5	0.25	4.1	0.29	7.5	0.54	8.1	0.26	2.07
Rock	22	1.5	0.11	14.8	1.06	16.3	1.17	5.1	0.16	7.14
SPAM Pennock	31	1.9	0.14	36.8	2.63	38.7	2.76	4.0	0.13	21.67
West Fork Sheep	36	1.9	0.14	6.5	0.47	8.5	0.60	6.2	0.20	3.04
Wigwam	37	4.6	0.33	158.4	11.31	163.0	11.63	4.7	0.15	76.17

Figure 1. Breakthrough curve of NH_4^+ in Corral Creek. Black points refer to theoretical conservative transport and blue points are measured concentrations from grab samples.

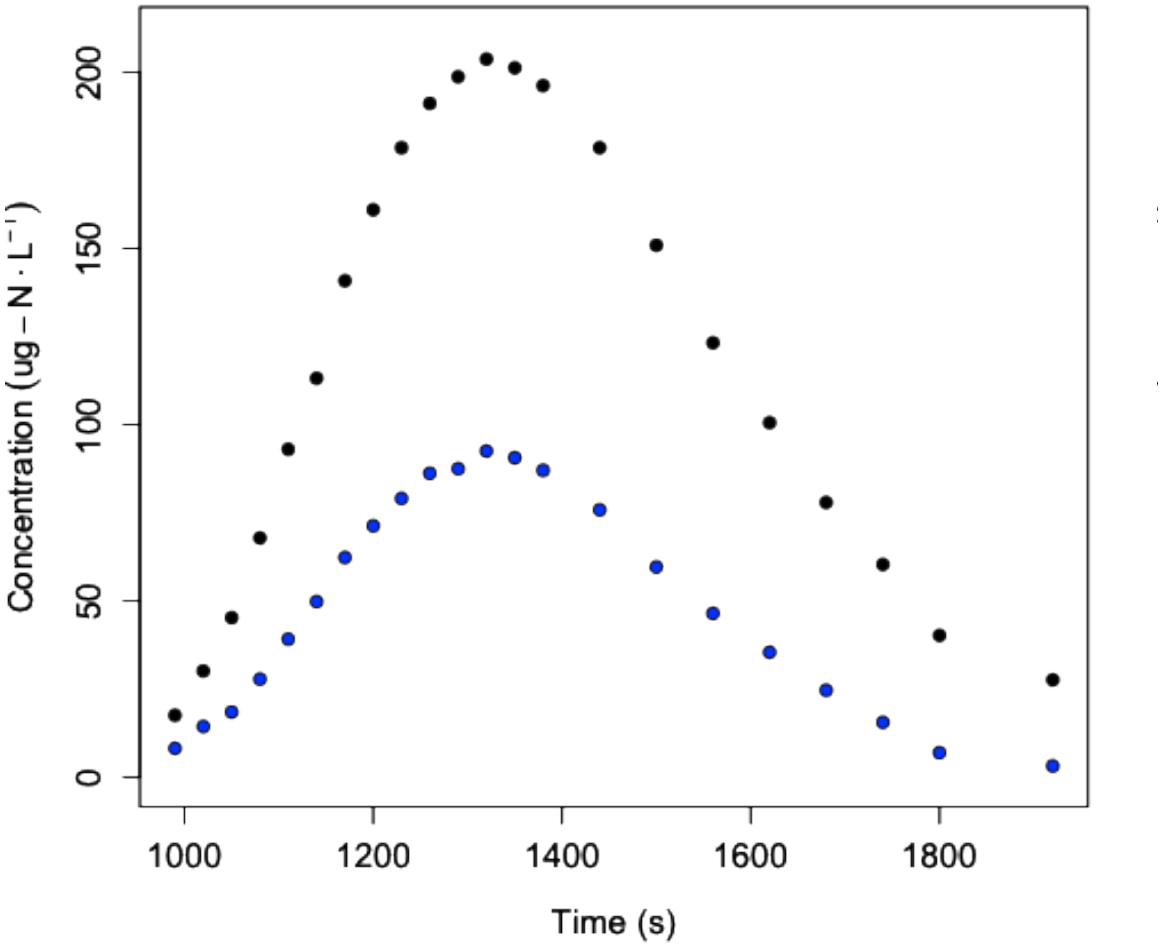

Figure 2. Estimating individual uptake lengths for each grab sample by determining longitudinal loss rates (k_L), where k_L is equal to the slope of the 2-point regression.

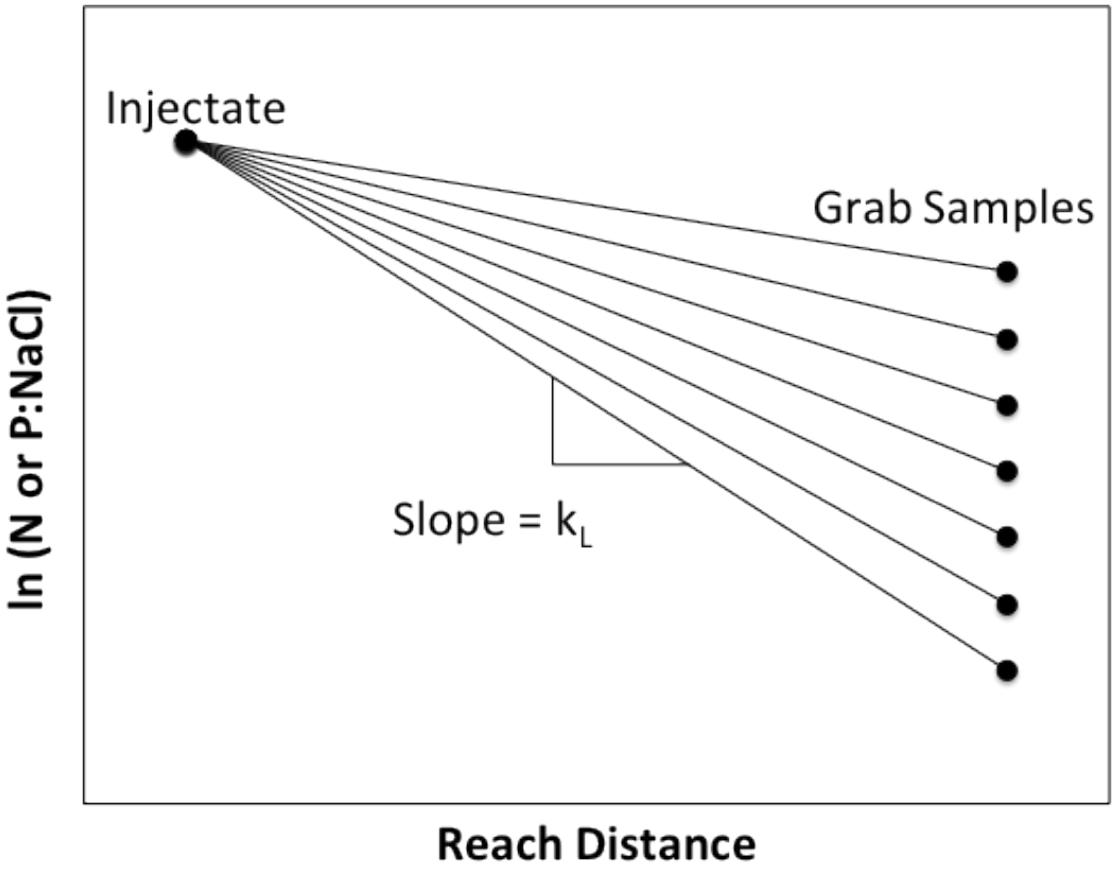

Figure 3. Determining ambient uptake lengths for each stream. Individual uptake lengths ($-1/k_L$) are plotted against their respective concentration and the linear regression is extrapolated.

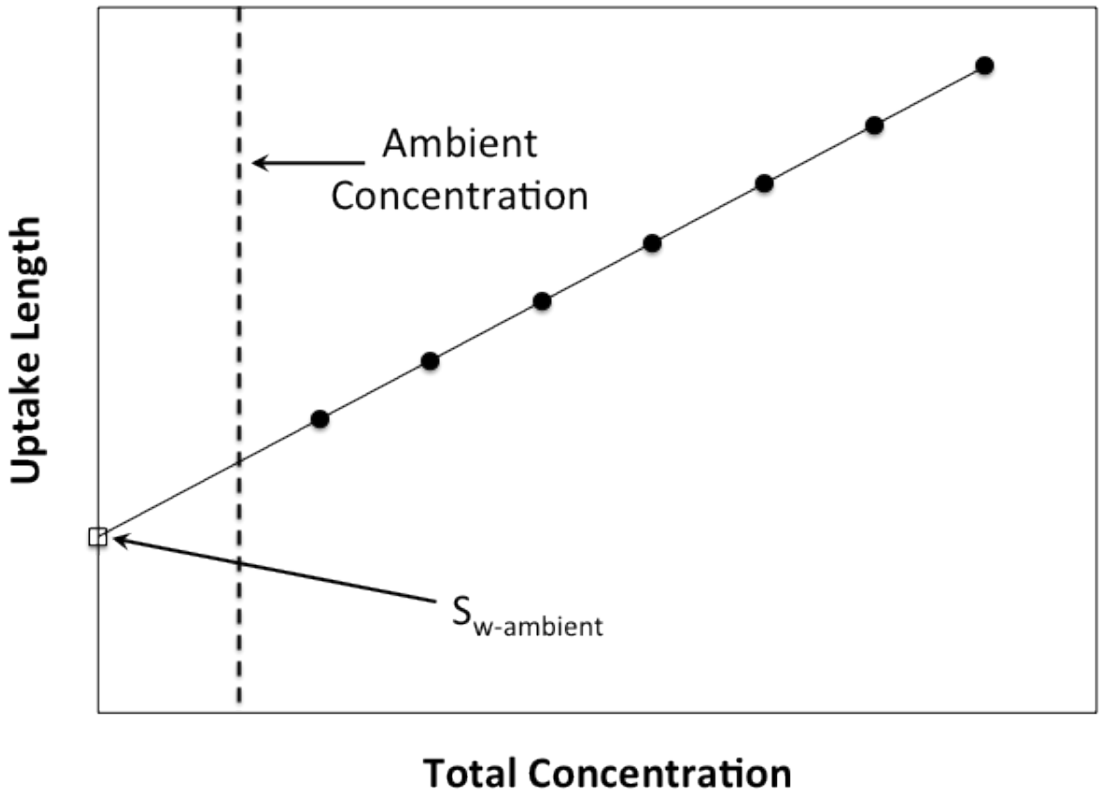

Figure 4. Estimating area under the nutrients breakthrough curve.

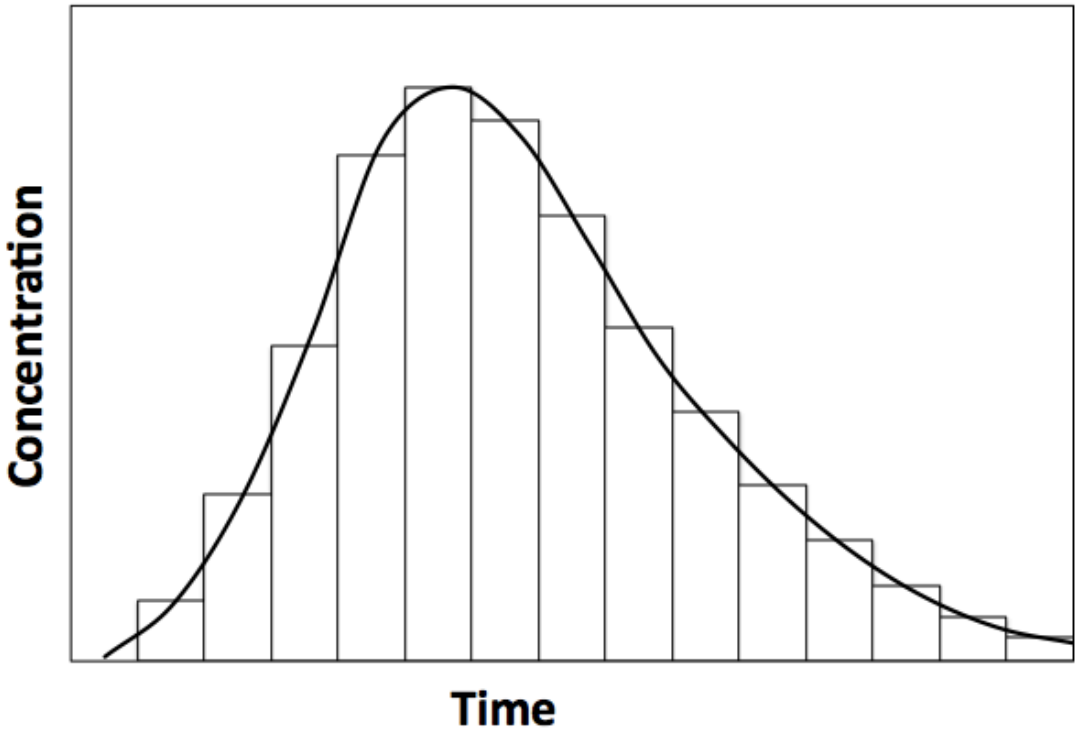

Figure 5a. Slug-time stream temperature as a function of altitude.

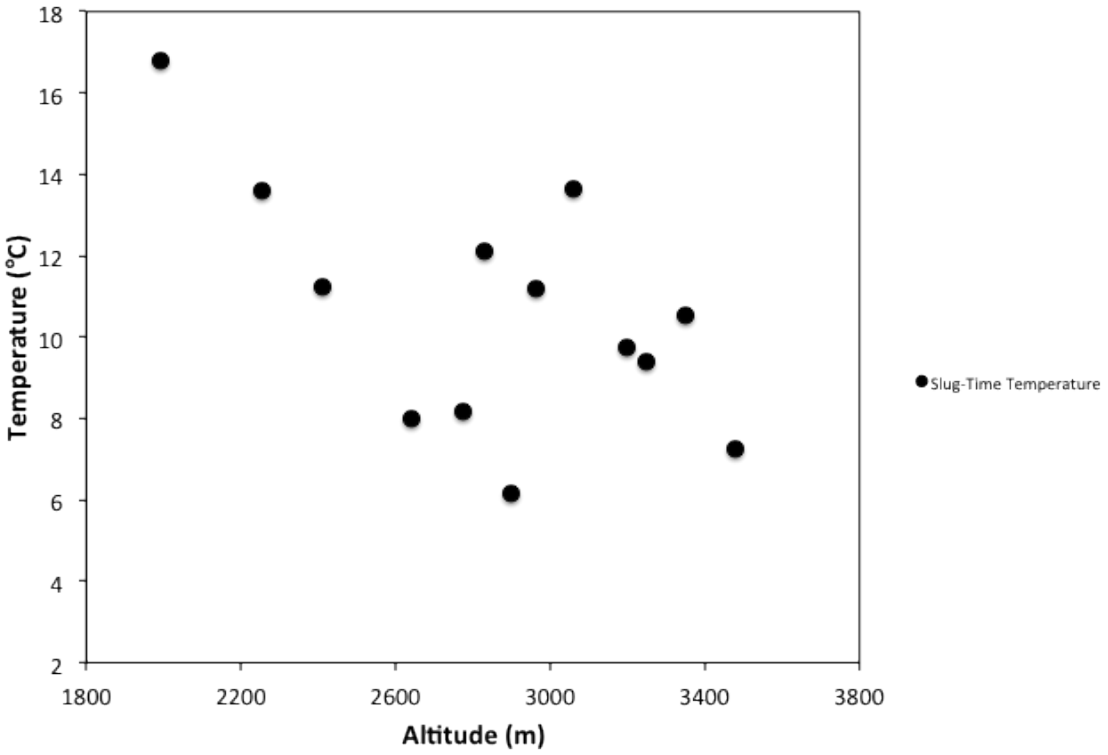

Figure 5b. 10-Day minimum temperature as a function of altitude.

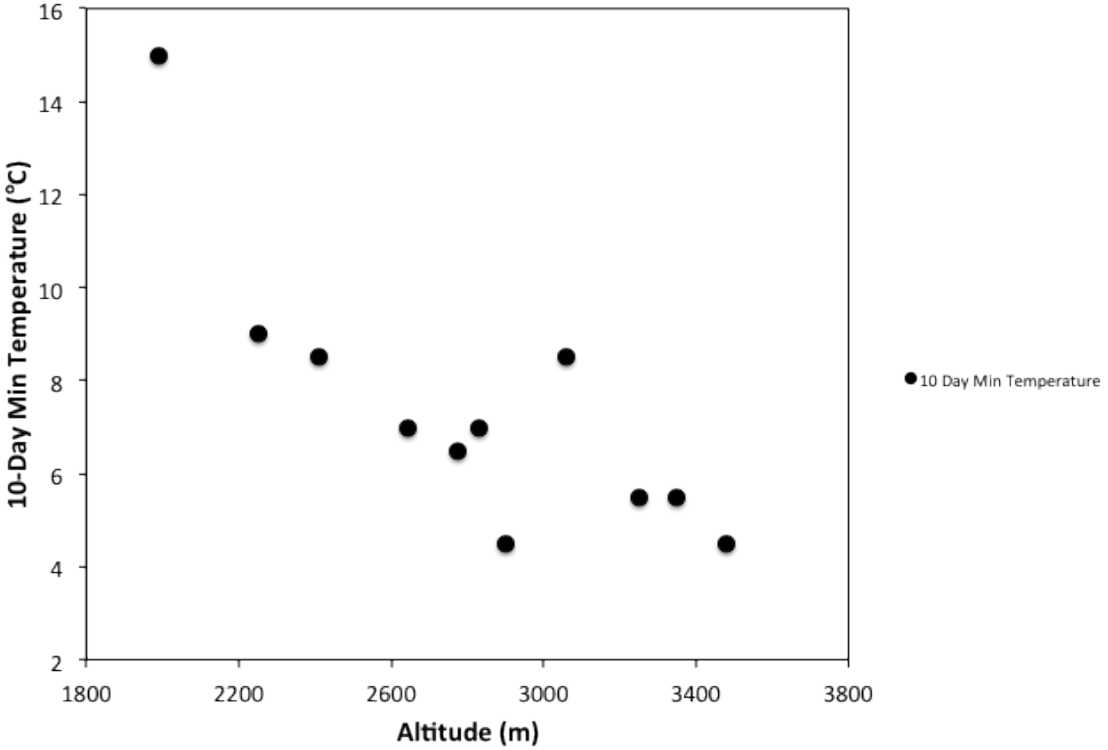

Figure 6. % Canopy cover as a function of altitude.

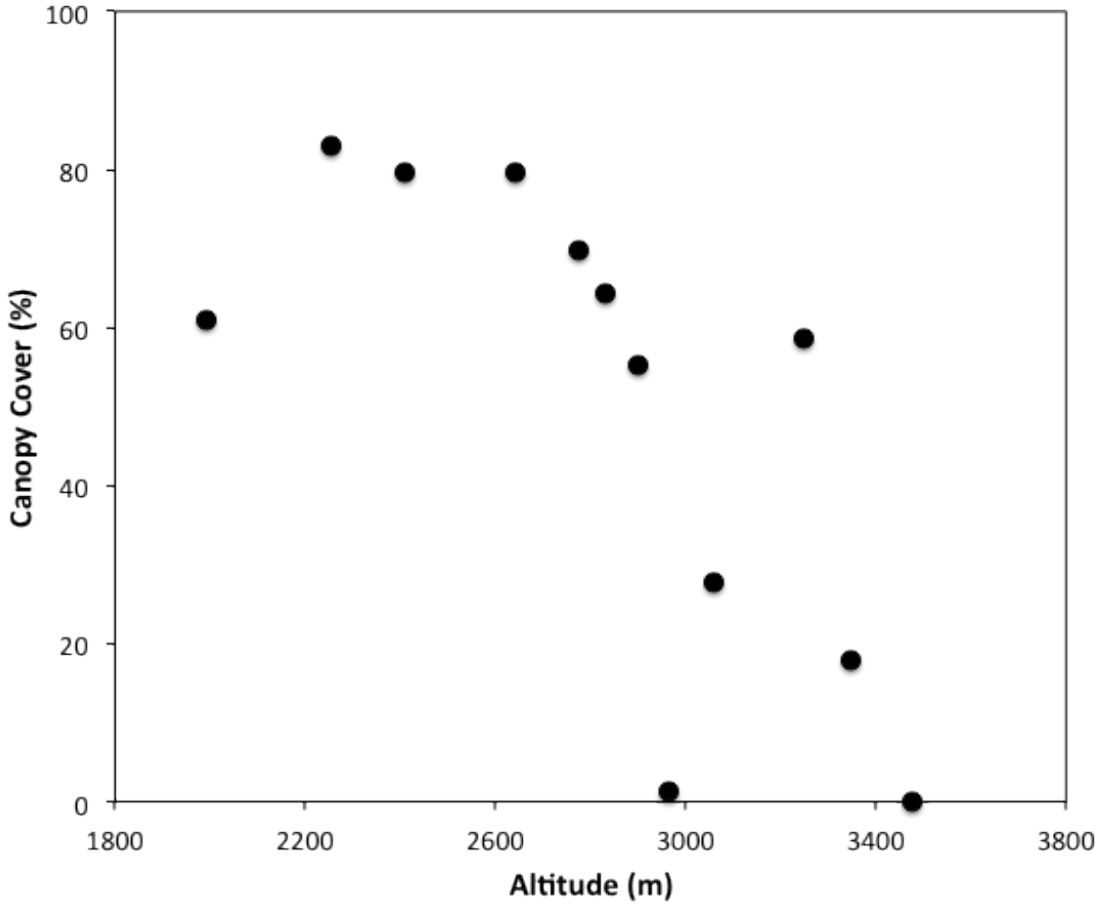

Figure 7a. Chlorophyll-**a** concentration as a function of altitude.

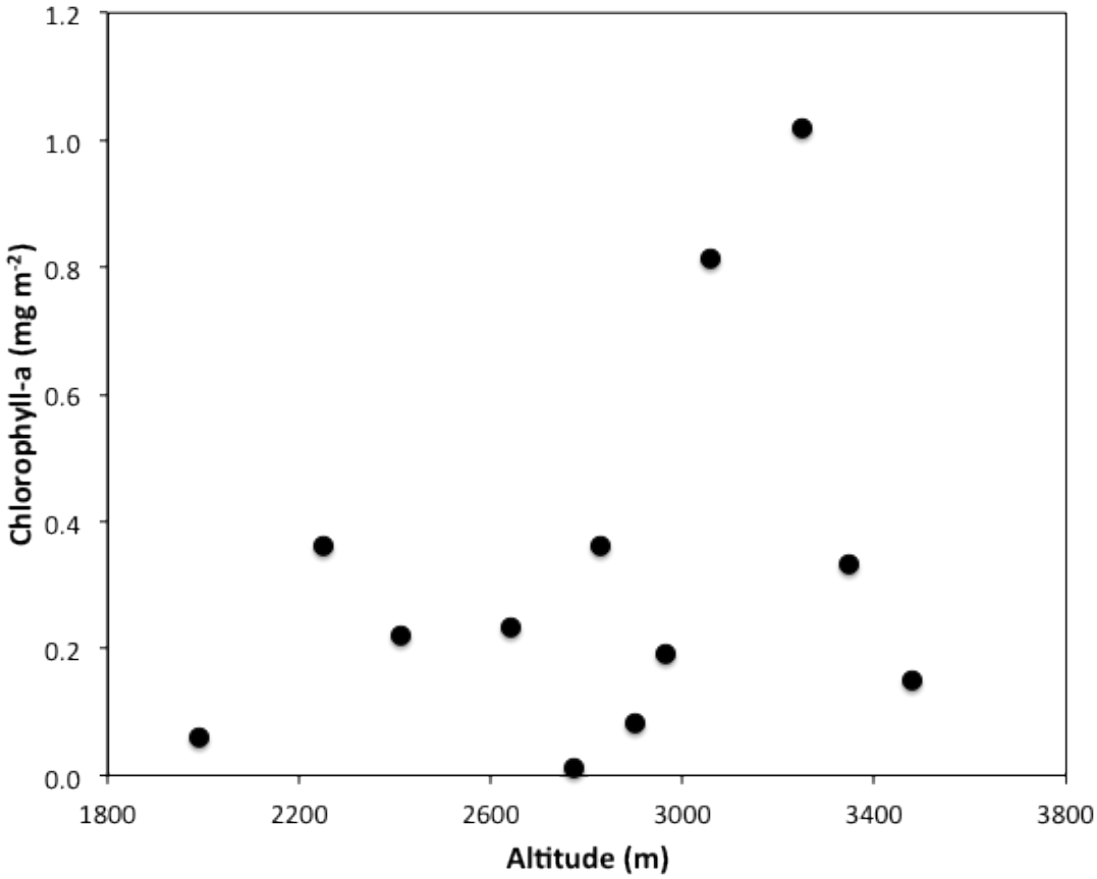

Figure 7b. Chlorophyll-**a** concentration as a function of temperature. Filled circles represent slug temperatures and open circles represent 10-day minimum temperatures.

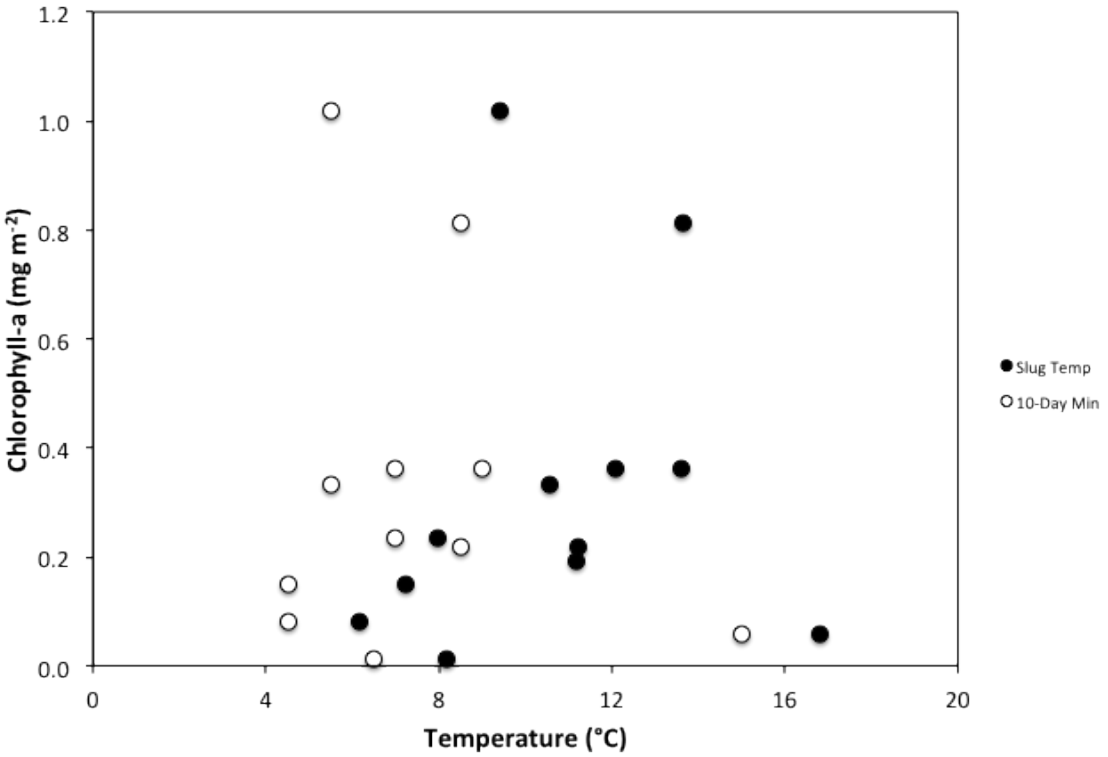

Figure 7c. Chlorophyll-**a** concentration as a function of % canopy cover.

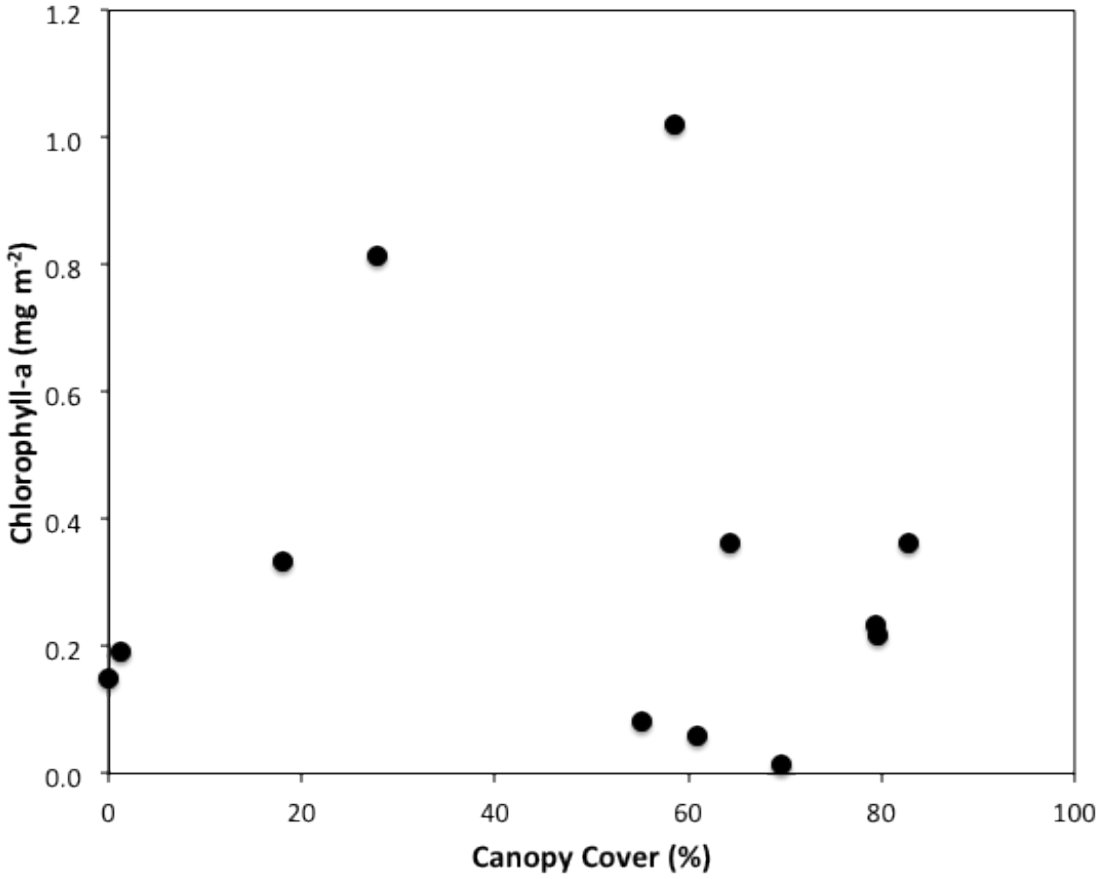

Figure 8. DIN:SRP molar ratio as a function of 10-day minimum temperature. Dotted line represents Redfield Ratio (DIN:SRP = 16).

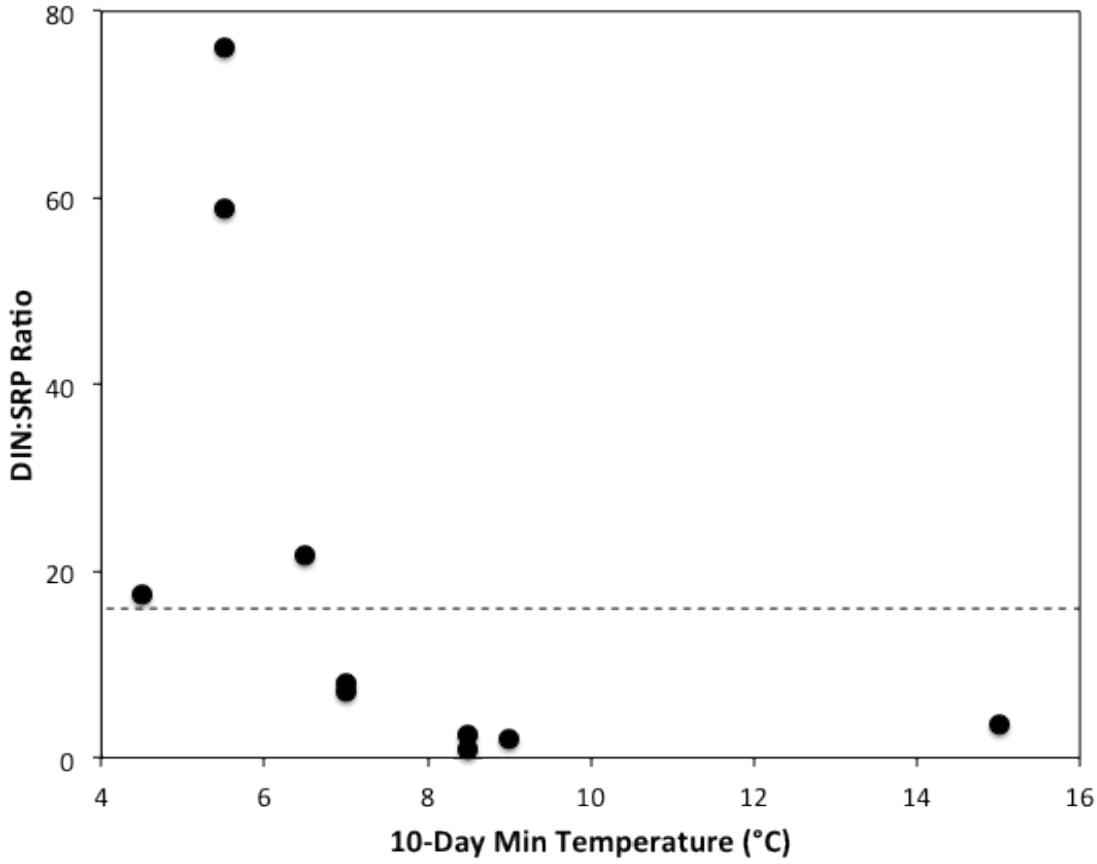

Figure 9. Individual NH_4^+ uptake lengths as a function of concentration in Corral Creek. Black circles represent samples from the ascending limb and open circles represent samples from the descending limb of the breakthrough curve.

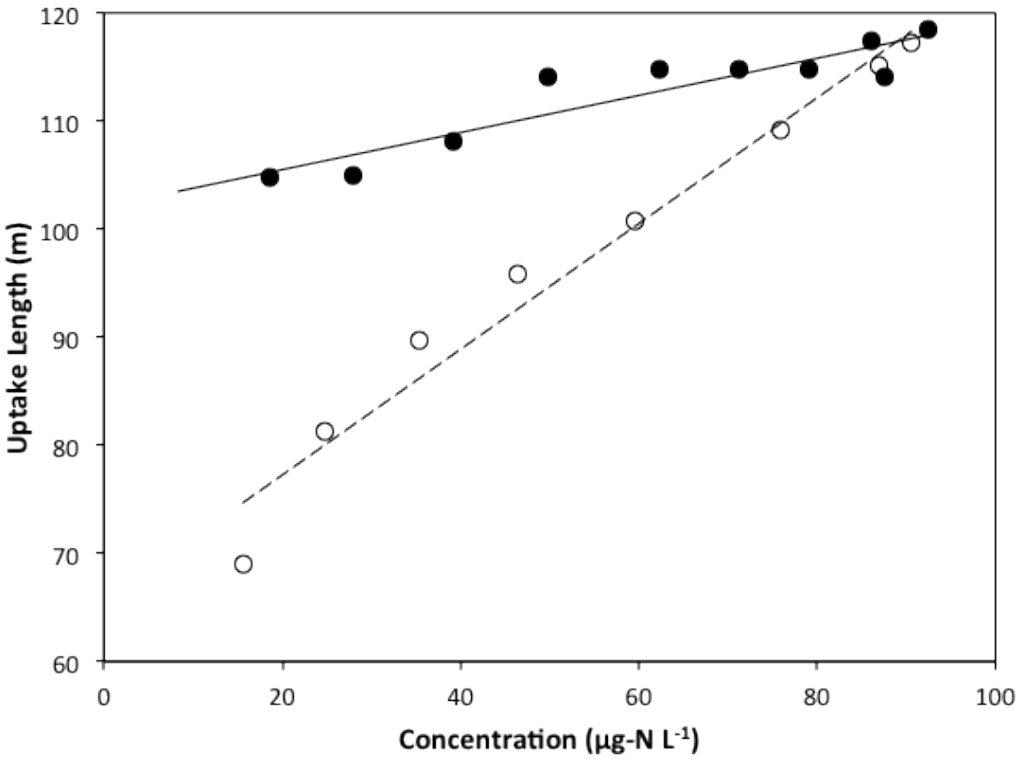

Figure 10a. NH_4^+ uptake rates versus 10-day minimum temperatures. Points represent TASCC uptake rates and error bars extend out toward ascending and descending uptake rates. The solid line is the linear regression through TASCC rates, the dash/dot line is the linear regression through ascending uptake rates, and the dotted line is the linear regression through descending uptake rates.

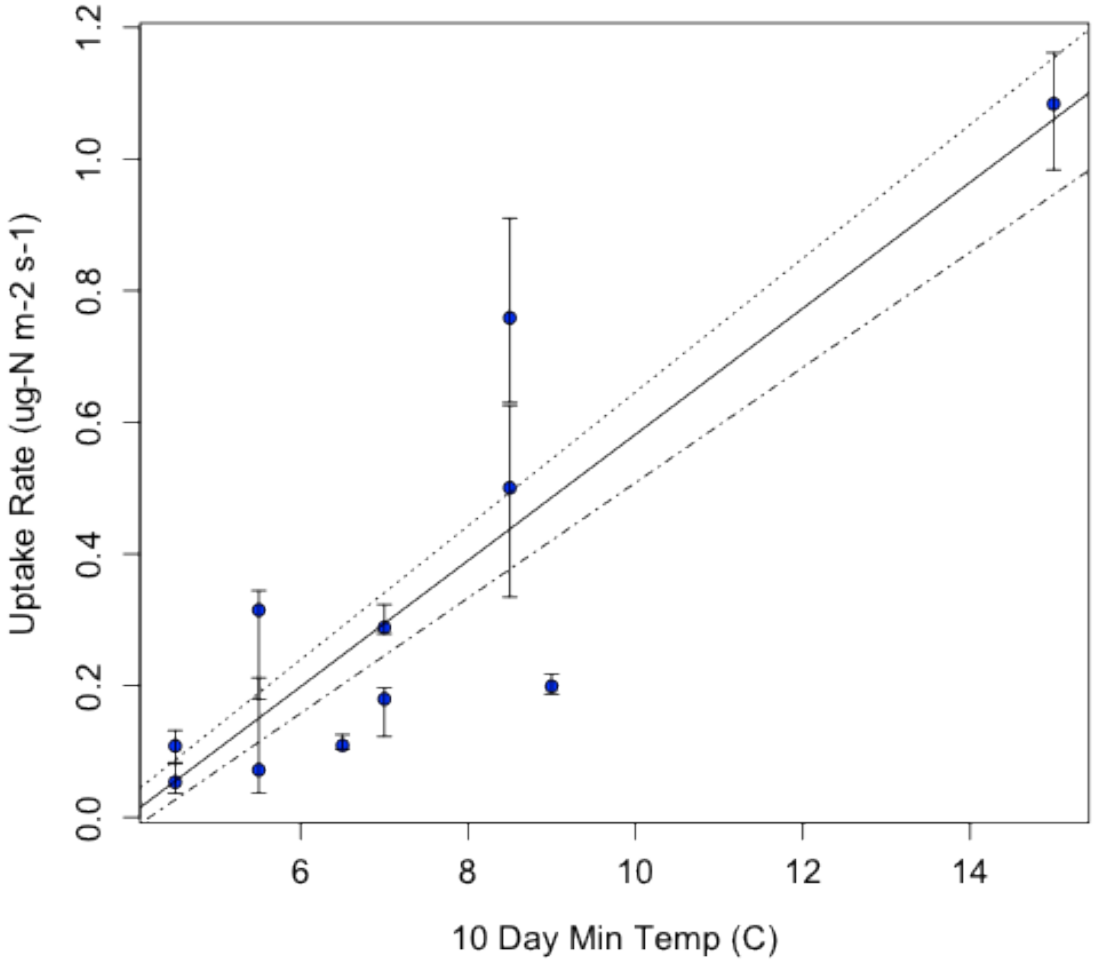

Figure 10b. NO_3^- uptake rates versus 10-day minimum temperatures. Points represent TASCC uptake rates and error bars extend out toward ascending and descending uptake rates. The solid line is the linear regression through TASCC rates, the dash/dot line is the linear regression through ascending uptake rates, and the dotted line is the linear regression through descending uptake rates.

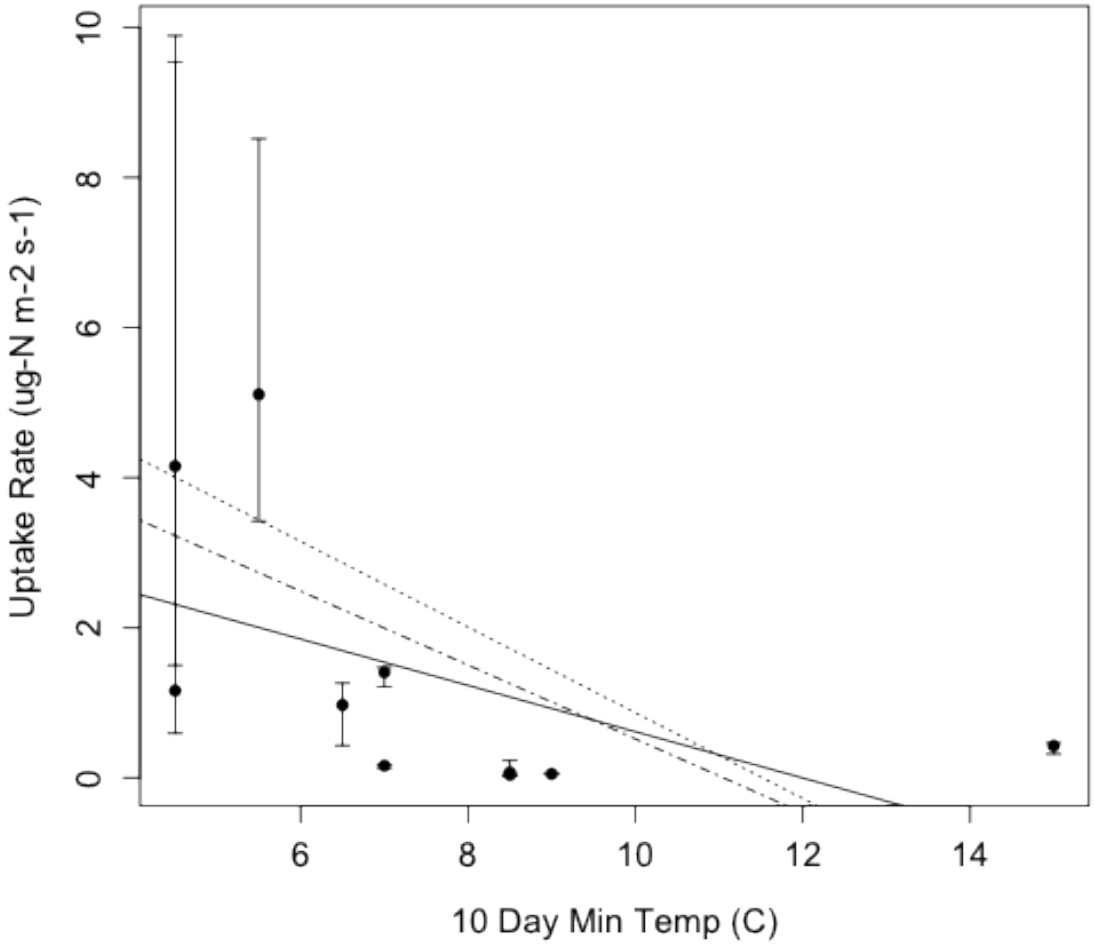

Figure 10c. SRP uptake rates versus 10-day minimum temperatures. Points represent TASCC uptake rates and error bars extend out toward ascending and descending uptake rates. The solid line is the linear regression through TASCC rates, the dash/dot line is the linear regression through ascending uptake rates, and the dotted line is the linear regression through descending uptake rates.

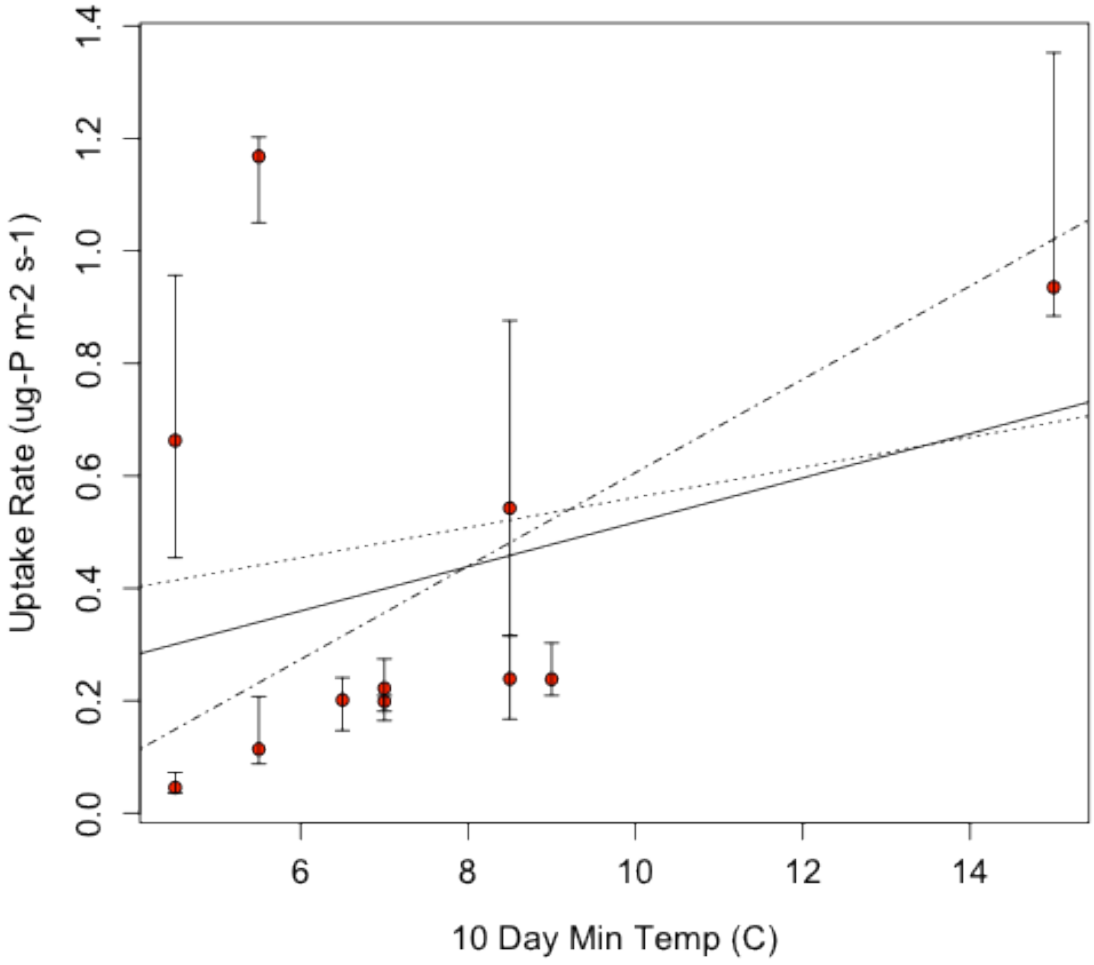

Figure 11a. Range in NH_4^+ uptake velocity (absolute value of ascending V_f minus descending V_f) as a function of A_S/A.

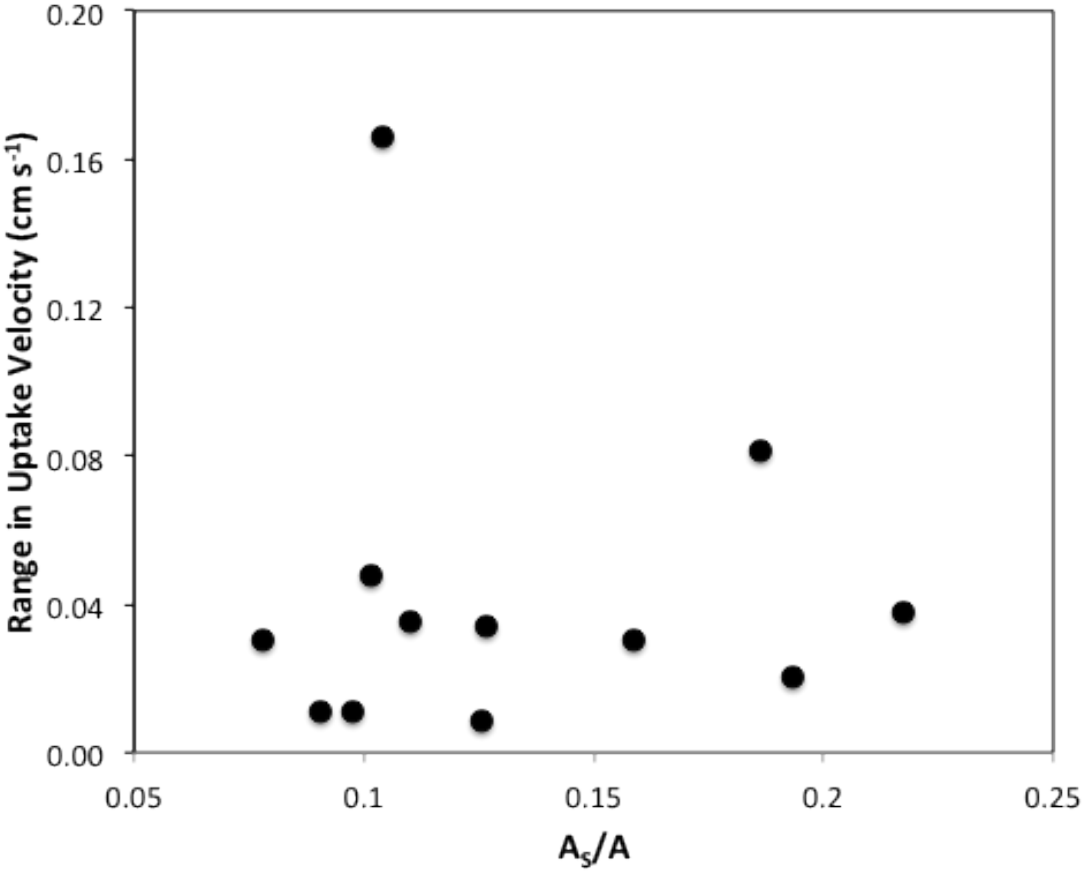

Figure 11b. Range in NO_3^- uptake velocity (absolute value of ascending V_f minus descending V_f) as a function of A_S/A.

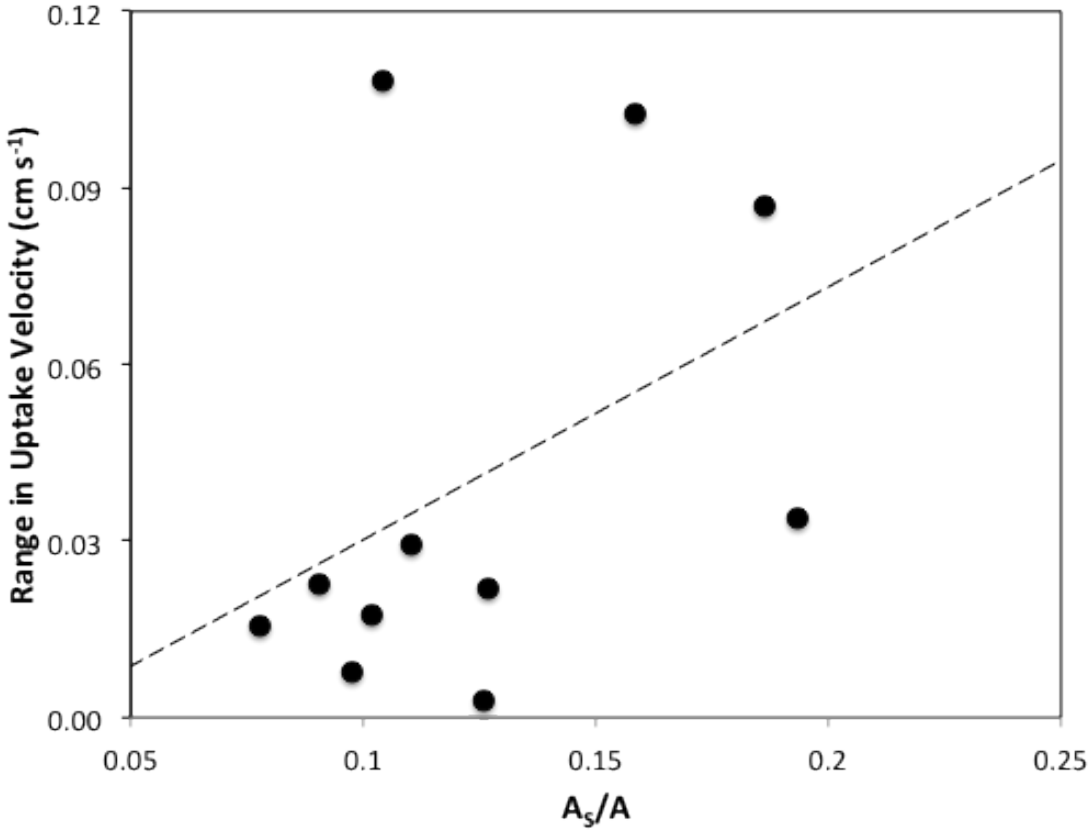

Figure 11c. Range in SRP uptake velocity (absolute value of ascending V_f minus descending V_f) as a function of A_S/A.

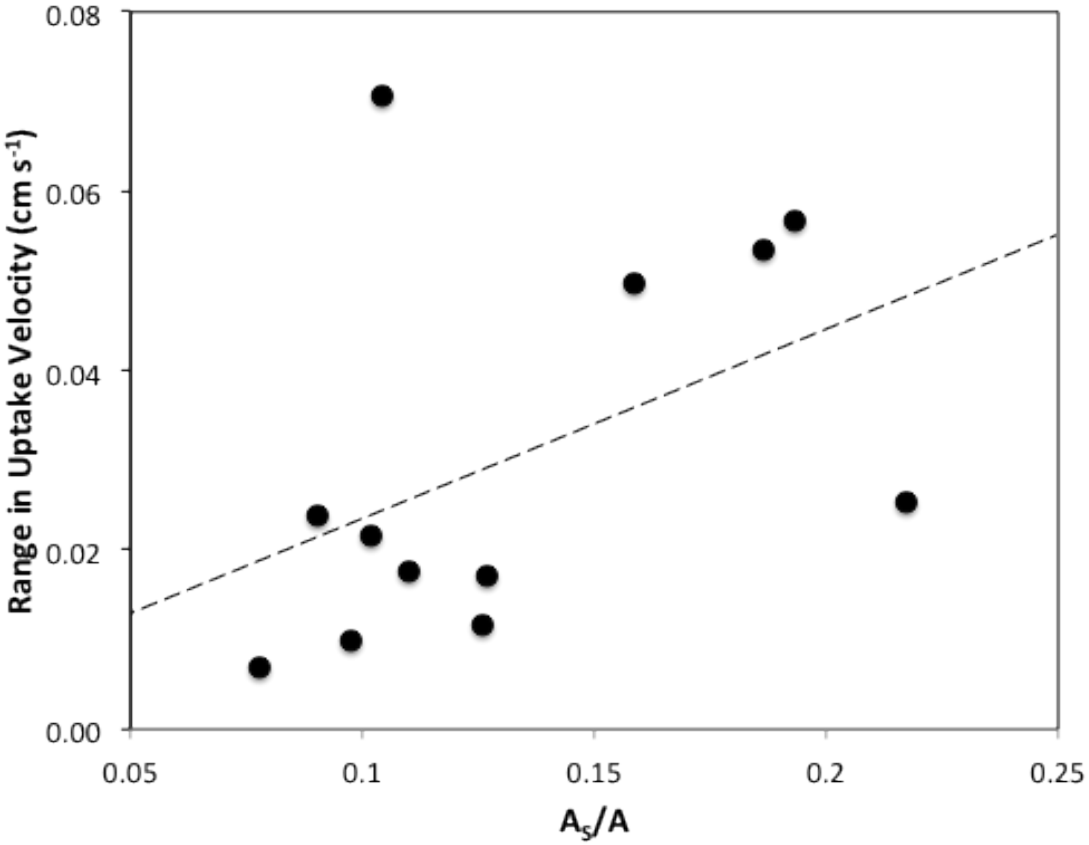

Figure 12a. Ascending NH_4^+ uptake velocity as a function of 10-day minimum temperature.

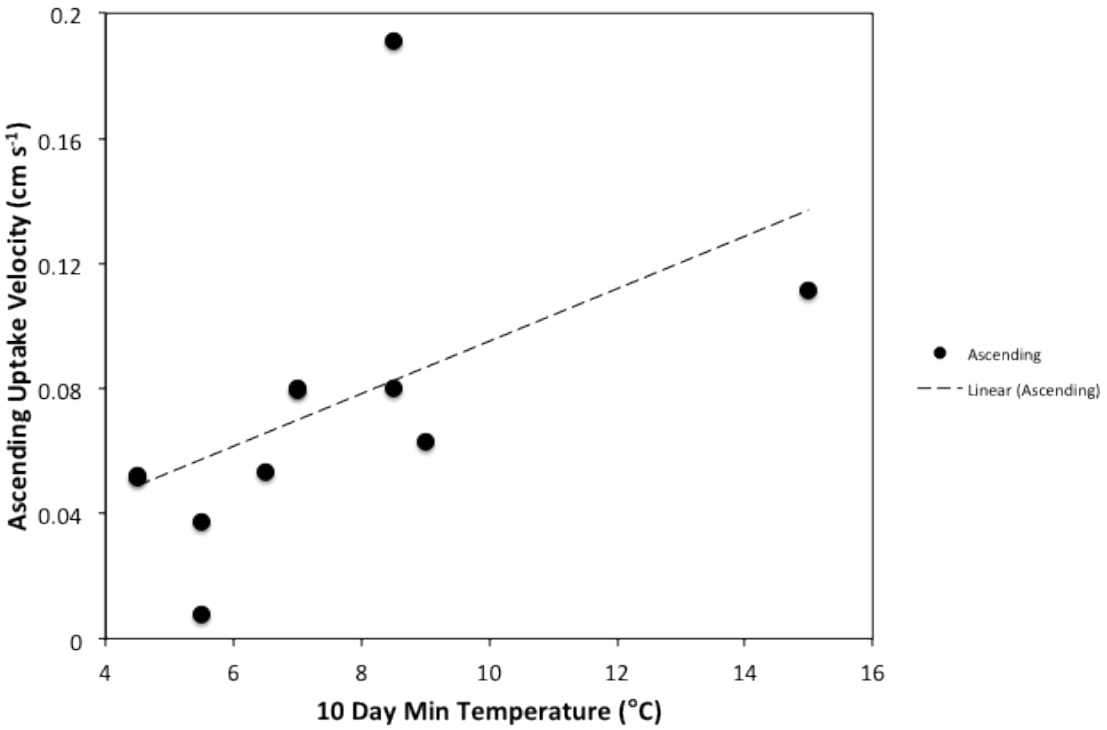

Figure 12b. Ascending NO_3^- uptake velocity as a function of 10-day minimum temperature.

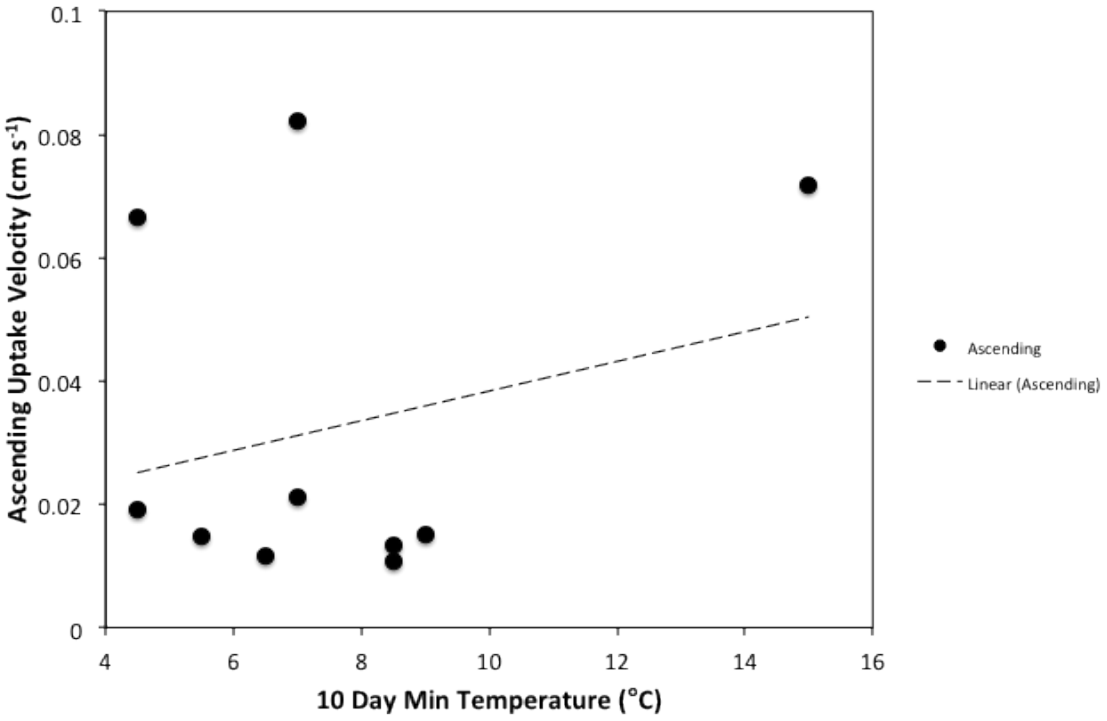

Figure 12c. Ascending SRP uptake velocity as a function of 10-day minimum temperature.

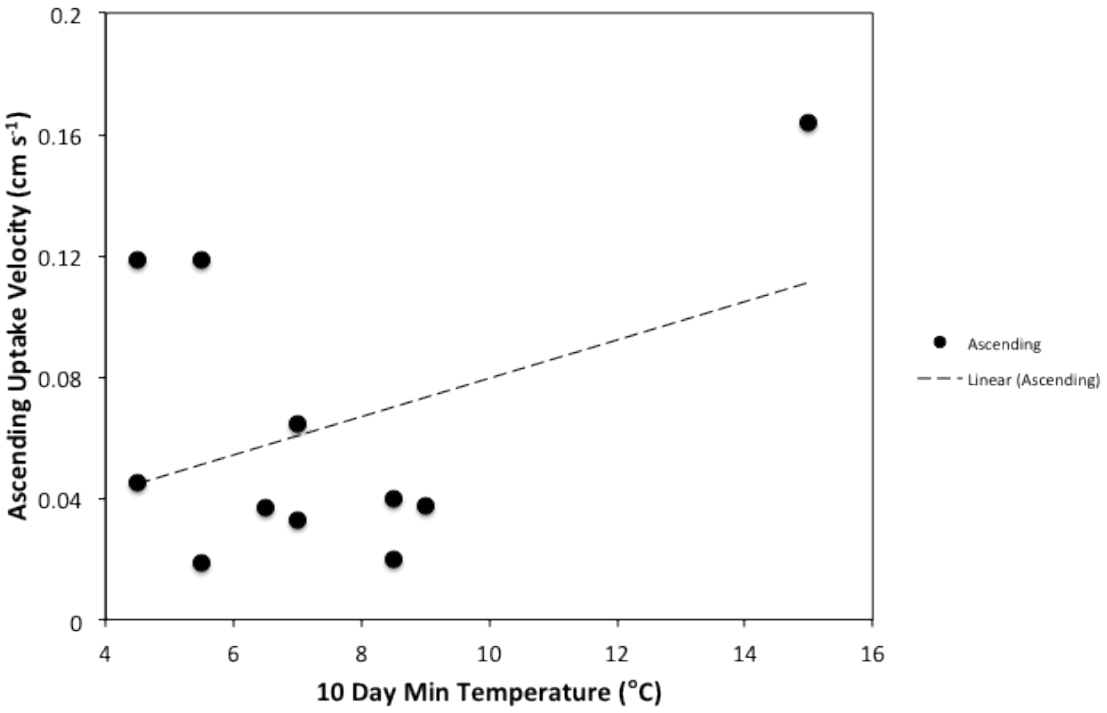

Figure 13. Ascending NH_4^+ uptake velocity as a function of N:P molar ratio.

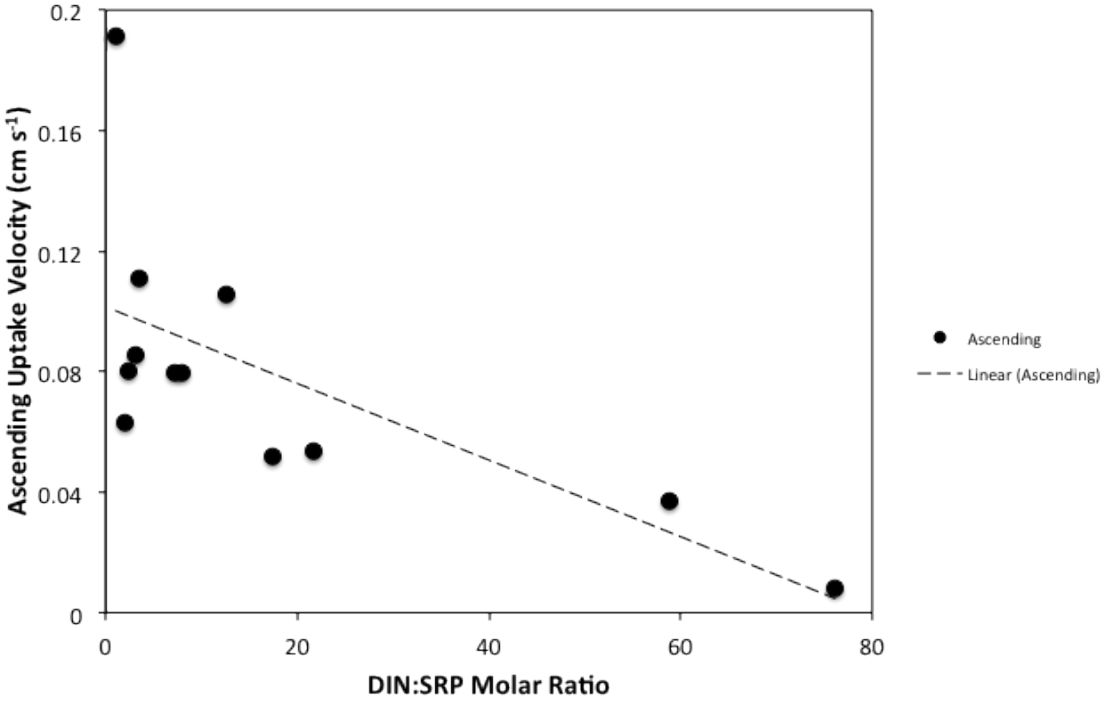

Figure 14a. Ascending NH_4^+ uptake rate as a function of altitude.

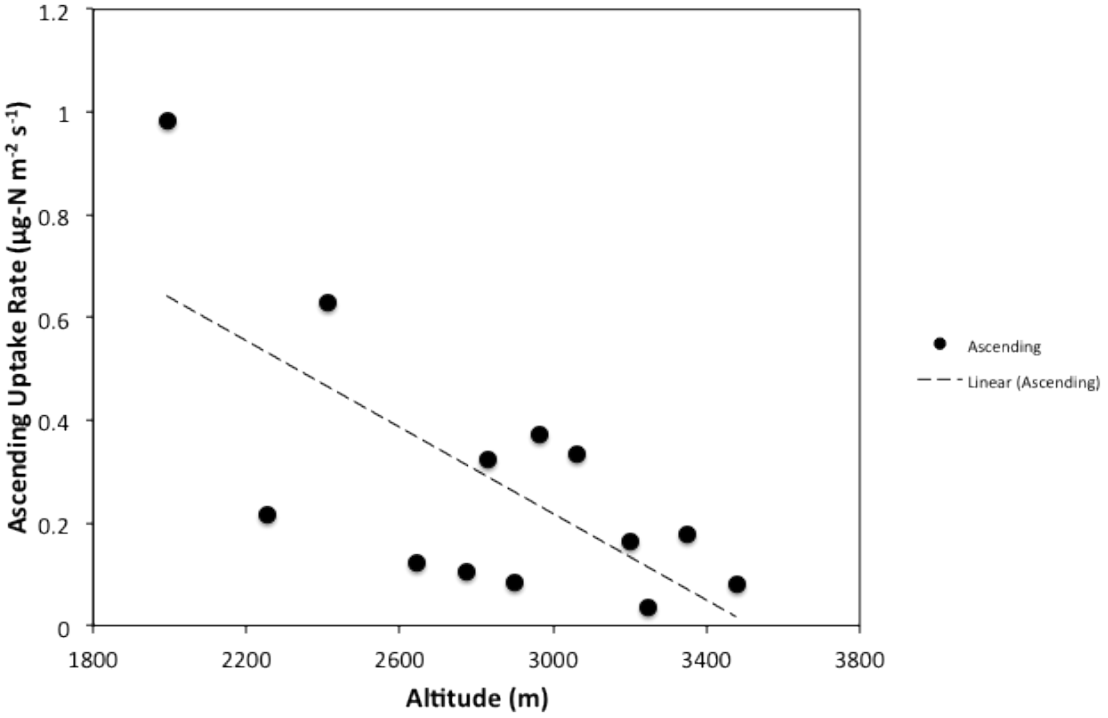

Figure 14b. Ascending NO_3^- uptake rate as a function of altitude.

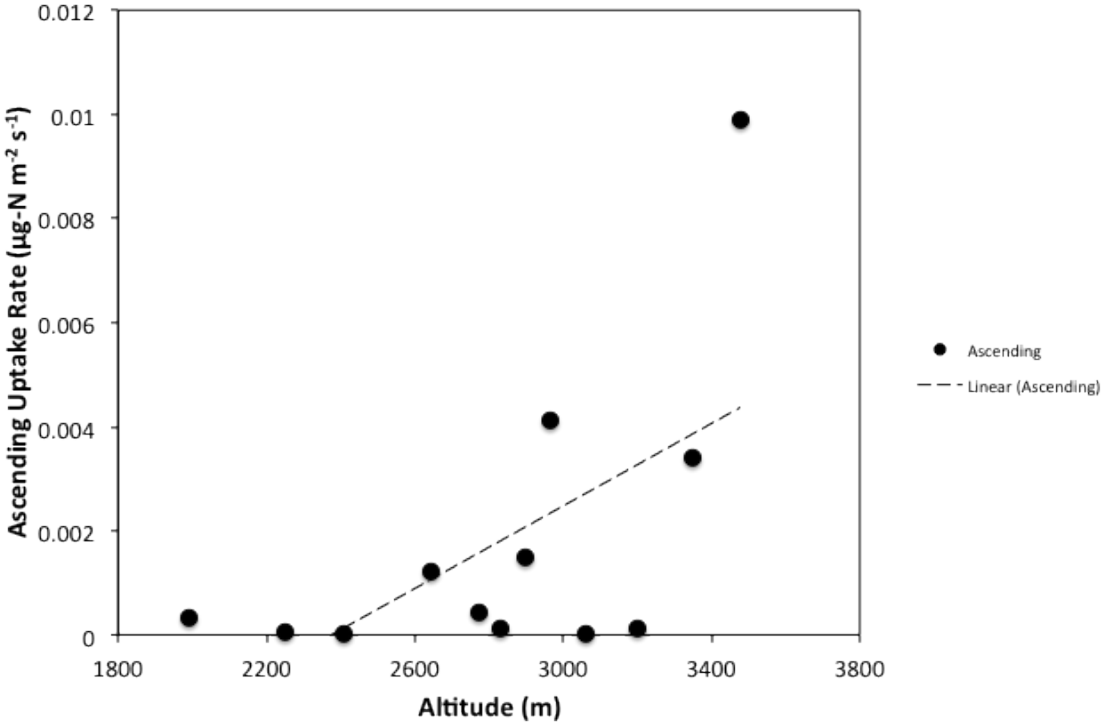

Figure 14c. Ascending SRP uptake rate as a function of altitude.

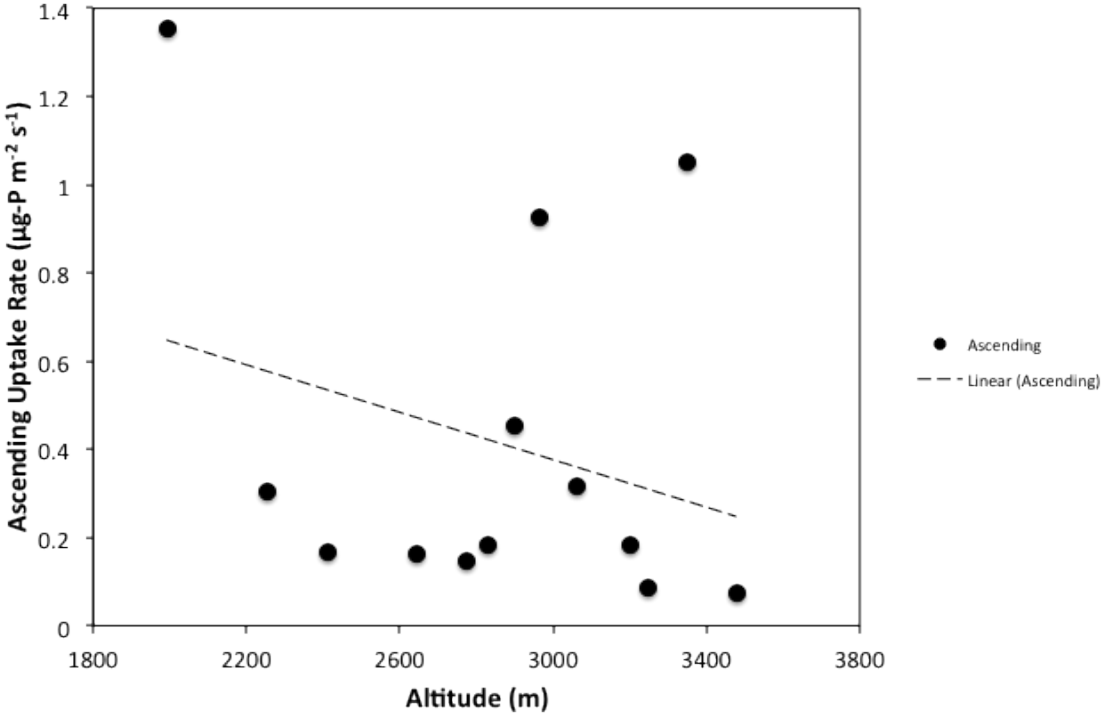

Figure 15a. Ascending NH_4^+ uptake rate as a function of 10-day minimum temperature.

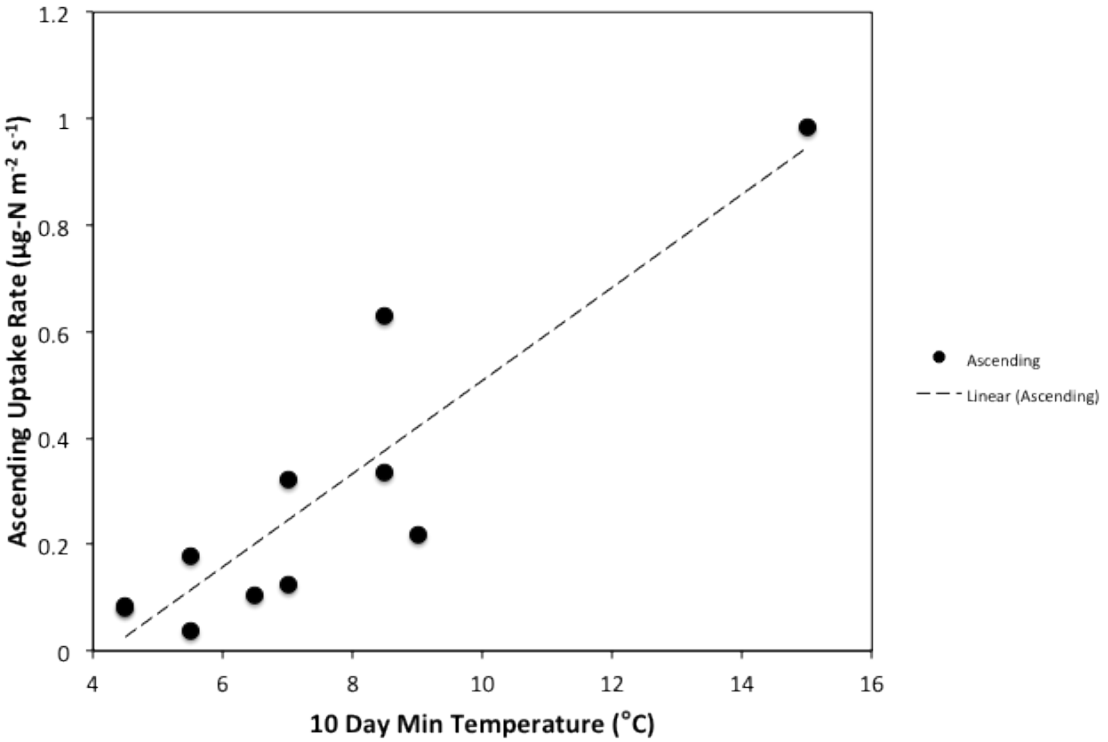

Figure 15b. Mass balance NO_3^- uptake rate as a function of 10-day minimum temperature.

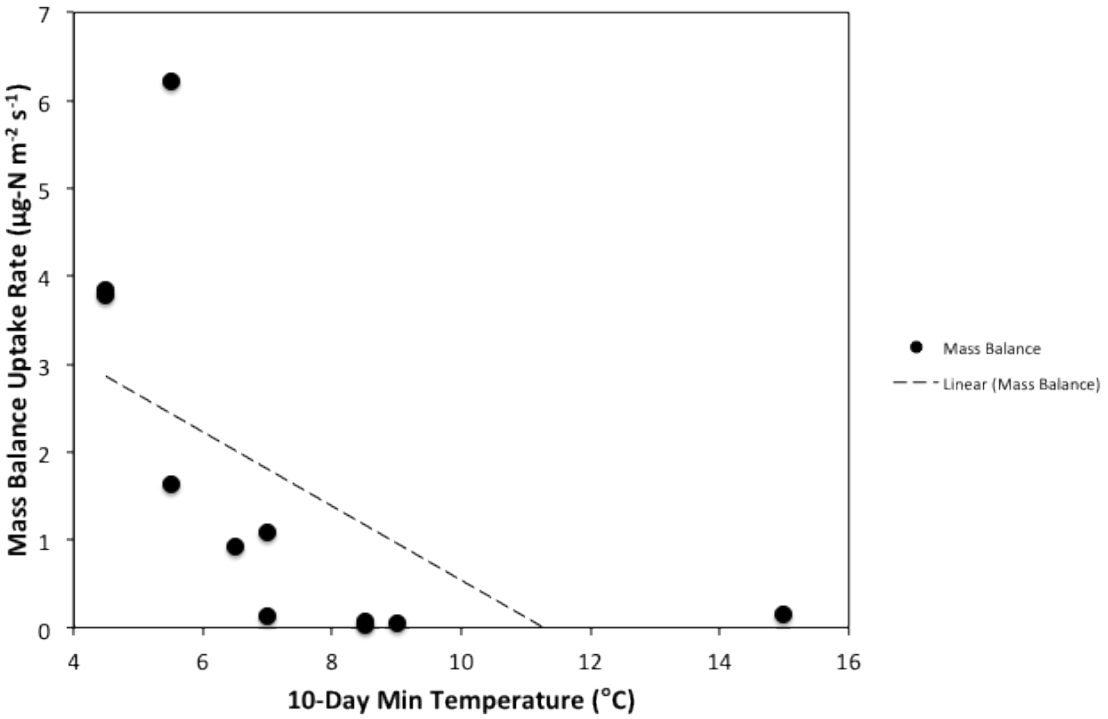

Figure 15c. Ascending SRP uptake rate as a function of 10-day minimum temperature.

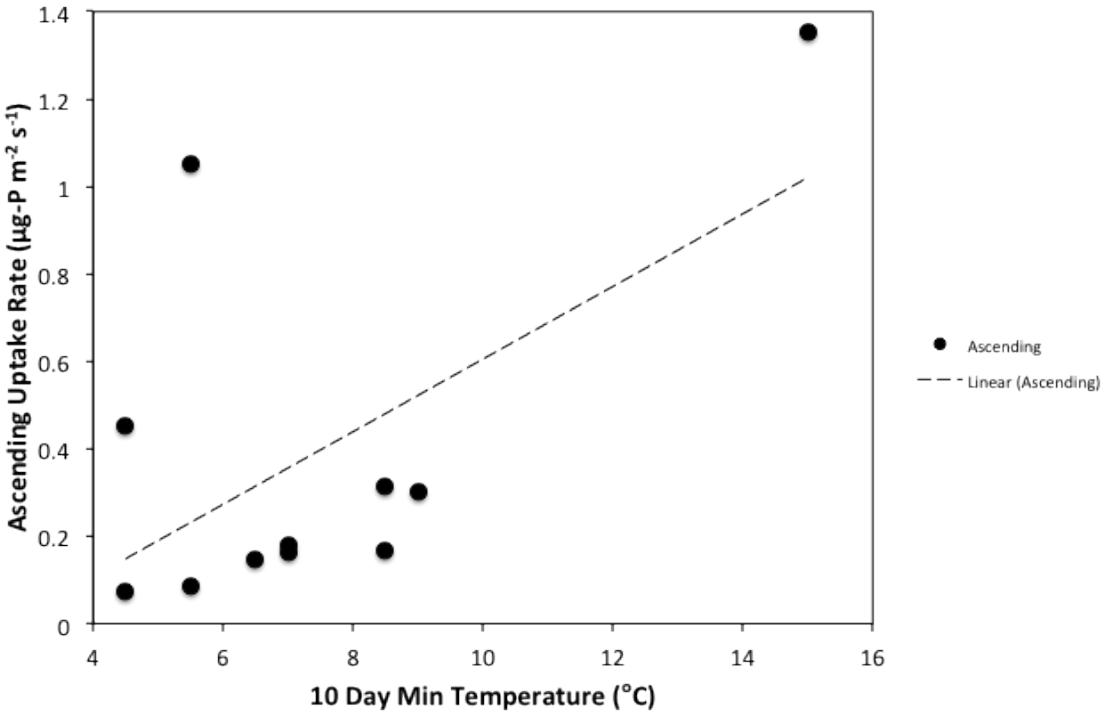

Figure 16a. Mass balance uptake rates versus TASCC uptake rates. Filled circles represent NH_4^+, open circles represent NO_3^-, and open squares represent SRP uptake rates. Dashed line represents 1:1 values.

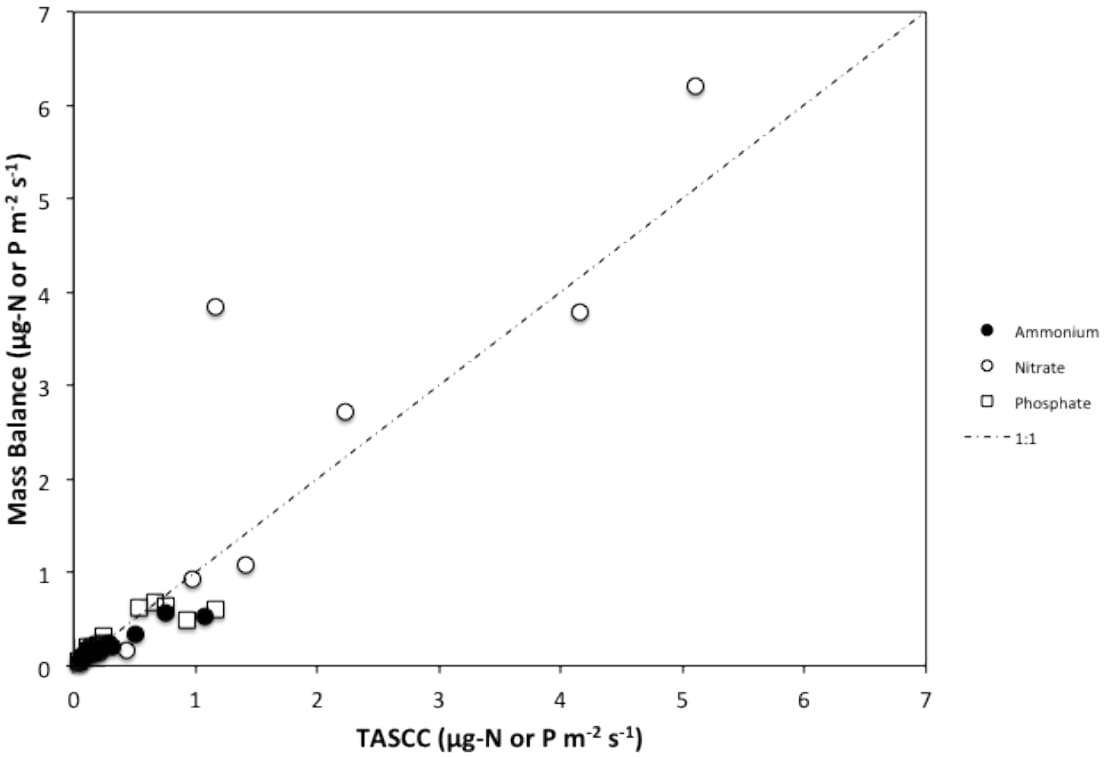

Figure 16b. Mass balance uptake rates versus TASCC uptake rates, zoomed in to show lower quadrant. Filled circles represent NH_4^+, open circles represent NO_3^-, and open squares represent SRP uptake rates. Dashed line represents 1:1 values.

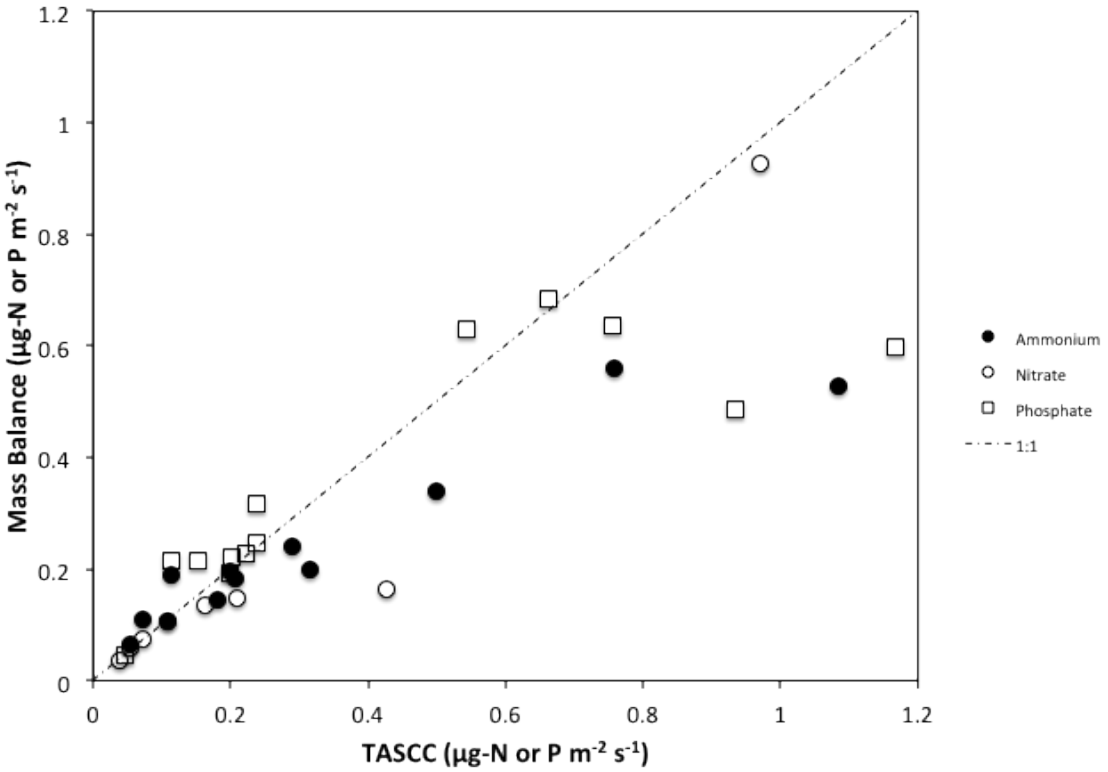

Figure 17a. Individual uptake rates of NH_4^+ as a function of concentration in Miller Fork, fit with a Michaelis-Menten curve.

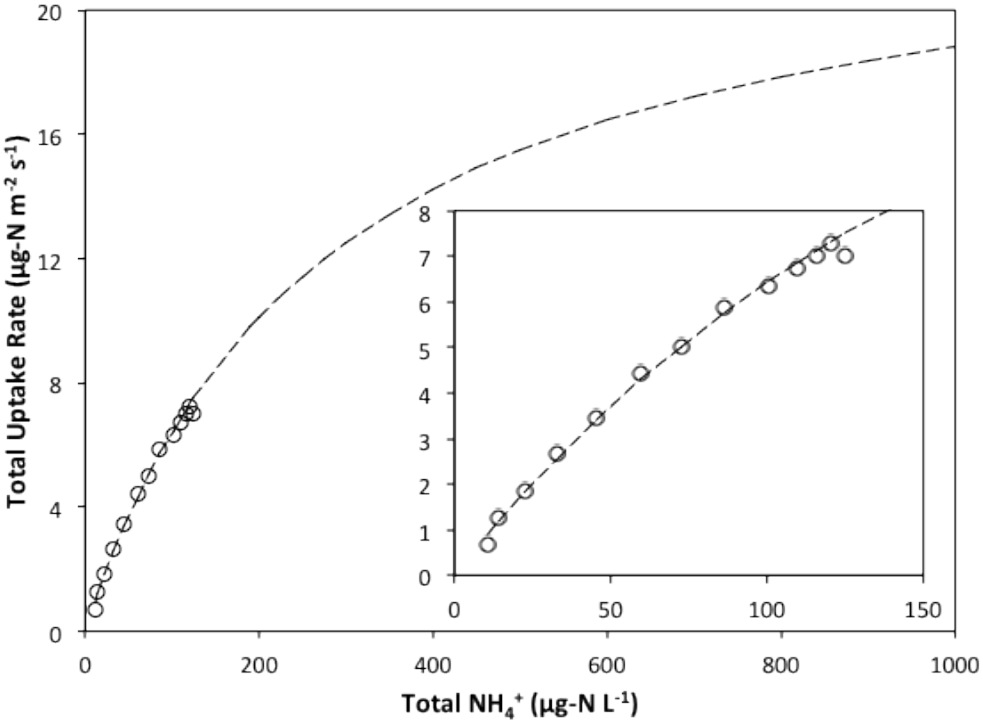

Figure 17b. Individual uptake rates of NH_4^+ as a function of concentration in Black Canyon, fit with a linear regression.

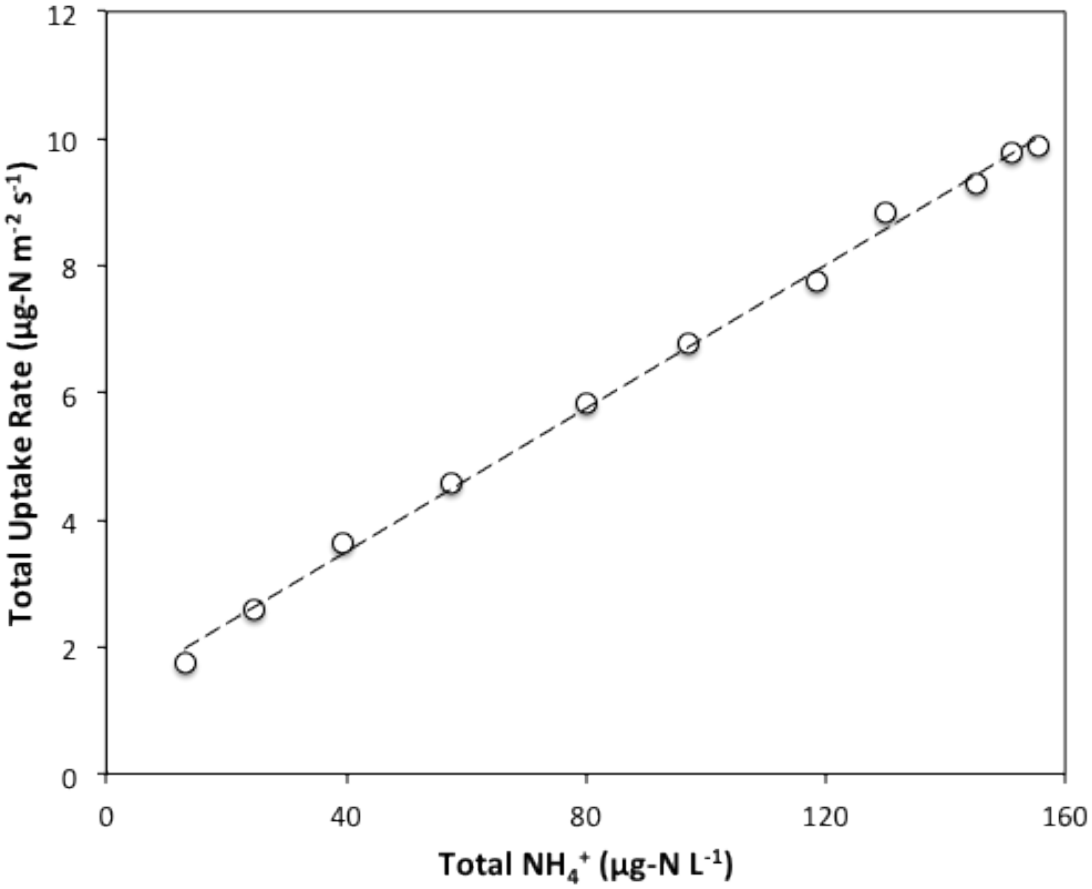

Figure 18a. NO_3^- response slope as a function of 10-day minimum temperature.

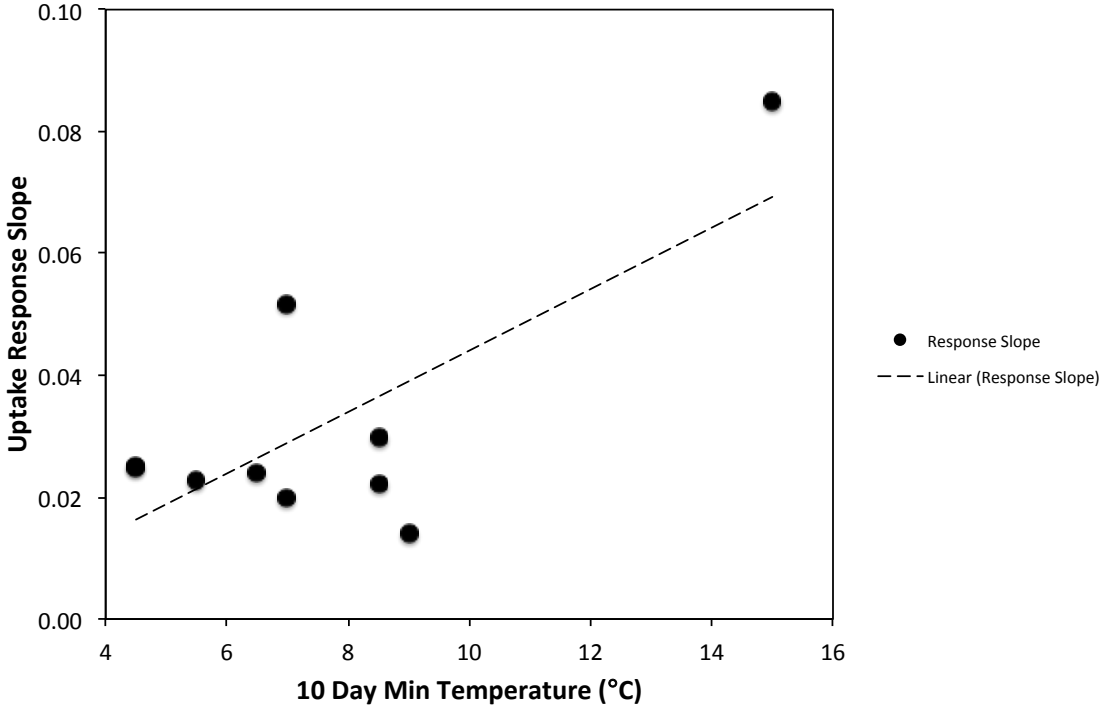

Figure 18b. NH_4^+ response slope as a function of 10-day minimum temperature.

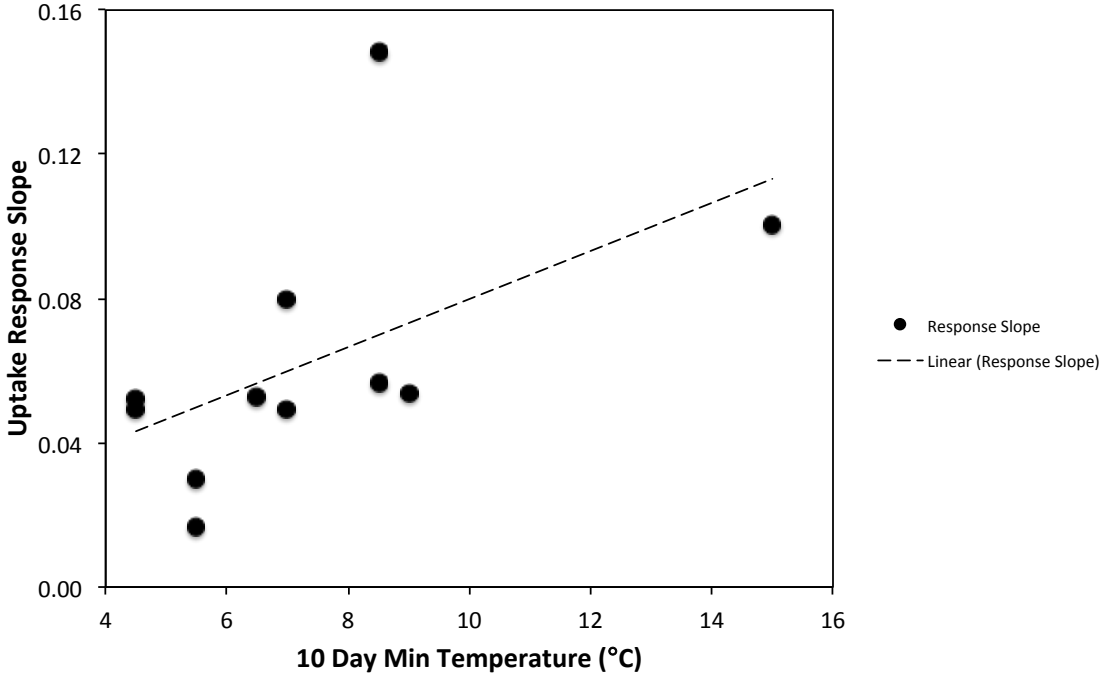

Figure 18c. SRP response slope as a function of 10-day minimum temperature.